SIAM J. IMAGING SCIENCES
Vol. 7, No. 4, pp. 2448–2487

Stein Unbiased GrAdient estimator of the Risk (SUGAR) for Multiple Parameter Selection*

Charles-Alban Deledalle†, Samuel Vaiter‡, Jalal Fadili§, and Gabriel Peyré‡

Abstract. Algorithms for solving variational regularization of ill-posed inverse problems usually involve operators that depend on a collection of continuous parameters. When the operators enjoy some (local) regularity, these parameters can be selected using the so-called Stein Unbiased Risk Estimator (SURE). While this selection is usually performed by an exhaustive search, we address in this work the problem of using the SURE to efficiently optimize for a collection of continuous parameters of the model. When considering nonsmooth regularizers, such as the popular ℓ_1-norm corresponding to soft-thresholding mapping, the SURE is a discontinuous function of the parameters preventing the use of gradient descent optimization techniques. Instead, we focus on an approximation of the SURE based on finite differences as proposed by Ramani and Unser for the Monte-Carlo SURE approach. Under mild assumptions on the estimation mapping, we show that this approximation is a weakly differentiable function of the parameters and its weak gradient, coined the Stein Unbiased GrAdient estimator of the Risk (SUGAR), provides an asymptotically (with respect to the data dimension) unbiased estimate of the gradient of the risk. Moreover, in the particular case of soft-thresholding, it is proved to also be a consistent estimator. This gradient estimate can then be used as a basis for performing a quasi-Newton optimization. The computation of the SUGAR relies on the closed-form (weak) differentiation of the nonsmooth function. We provide its expression for a large class of iterative methods including proximal splitting methods and apply our strategy to regularizations involving nonsmooth convex structured penalties. Illustrations of various image restoration and matrix completion problems are given.

Key words. inverse problems, risk estimation, SURE, parameter selection, proximal splitting, sparsity

AMS subject classifications. 68U10, 49N45, 65K10, 90C31

DOI. 10.1137/140968045

1. Introduction.

In this paper, we consider the recovery problem of a signal $x_0 \in \mathcal{X}$ (where $\mathcal{X} = \mathbb{R}^N$ or is a suitable finite-dimensional Hilbert space that can be identified to $\mathbb{R}^N$) from a realization $y \in \mathcal{Y} = \mathbb{R}^P$ of the normal random vector

$$Y = \mu_0 + W \quad \text{with} \quad \mu_0 = \Phi x_0, \tag{1.1}$$

where $W \sim \mathcal{N}(0, \sigma^2 \mathrm{Id}_P)$ and the linear imaging operator $\Phi : \mathcal{X} \to \mathcal{Y}$ entails some loss of information. Typically, $P = \dim(\mathcal{Y})$ is smaller than $N = \dim(\mathcal{X})$ or Φ is rank-deficient, and the recovery problem is ill-posed.

*Received by the editors May 6, 2014; accepted for publication (in revised form) August 19, 2014; published electronically November 25, 2014. This research was supported by the European Research Council (ERC project SIGMA-Vision).
http://www.siam.org/journals/siims/7-4/96804.html
†IMB, CNRS-Université Bordeaux, F-33405 Talence, France (charles-alban.deledalle@math.u-bordeaux1.fr). Part of this work was completed while this author was at CEREMADE.
‡CEREMADE, CNRS-Université Paris-Dauphine, Paris 75775, France (samuel.vaiter@ceremade.dauphine.fr, gabriel.peyre@ceremade.dauphine.fr).
§GREYC, CNRS-ENSICAEN-Université de Caen, 14050 Caen Cedex, France (jalal.fadili@greyc.ensicaen.fr).

Let $(y,\theta) \mapsto x(y,\theta)$ be some recovery mapping, possibly multivalued, which attempts to approach x_0 from a given realization $y \in \mathcal{Y}$ of Y and is parametrized by a collection of continuous parameters $\theta \in \Theta$. Throughout, Θ is considered as a subset of a linear subspace of dimension $\dim(\Theta)$. We also denote $\mu(y,\theta) = \Phi x(y,\theta) \in \mathcal{Y}$ and assume in the rest of the paper that it is always a single-valued mapping, though $x(y,\theta)$ may not be.

Depending on the smoothness of the mapping $y \mapsto \mu(y,\theta)$, the recovered estimate enjoys different regularity properties. For instance, $\mu(y,\theta)$ can be built by solving a variational problem with some regularizing penalty parametrized by θ (see the example in (1.2), as well as sections 4 and 5). This regularization is generally chosen so as to preserve/promote the interesting structure underlying x_0, e.g., singularities, textures, etc. Also, depending on its choice and that of the data fidelity, the resulting mapping $y \mapsto \mu(y,\theta)$ may be smooth or not. To cover most of these situations, throughout the paper, we will assume that $(y,\theta) \mapsto \mu(y,\theta)$ is *weakly differentiable* with respect to both the observation y and the collection of parameters θ.

Recall that for a locally integrable function $f : a \in \Omega \mapsto \mathbb{R}$, where Ω is an open subset of $\mathbb{R}^N$, its weak partial derivative with respect to a_i in Ω is the locally integrable function g_i on Ω such that

$$\int_\Omega g_i(a)\varphi(a)\mathrm{d}a = -\int_\Omega f(a)\frac{\partial\varphi(a)}{\partial a_i}\mathrm{d}a$$

holds for all functions $\varphi \in C_c^1(\Omega)$, i.e., the space of continuously differentiable functions of compact support. The weak partial derivative, if it exists, is uniquely defined Lebesgue-almost everywhere (-a.e.). Thus we write

$$g_i = \frac{\partial f}{\partial a_i},$$

and all such pointwise relations involving weak derivatives will accordingly be understood to hold Lebesgue-a.e. A function is said to be weakly differentiable if all its weak partial derivatives exist. Similarly, a vector-valued function $h : a \in \mathbb{R}^N \mapsto h(a) = (h_1(a),\dots,h_P(a)) \in \mathbb{R}^P$ is weakly differentiable if $h_k(a)$ is weakly differentiable for all $k \in \{1,\dots,P\}$, and we will denote by $\partial h(a)$ its weak Jacobian, and by $\nabla g(a) = \partial h(a)^*$ its adjoint. Remark that weak differentiation concepts boil down to the classical ones when the considered function is $\mathcal{C}^1$. A comprehensive account on weak differentiability can be found in, e.g., [29, 31].

Getting back to the estimator $x(y,\theta)$, we now discuss some typical examples covered in this paper.

- Given (y,θ), consider a minimizer of a convex variational problem of the form

$$x(y,\theta) = \operatorname*{Argmin}_{x\in\mathcal{X}} \{E(x,y,\theta) = H(y,\Phi x) + R(x,\theta)\}, \tag{1.2}$$

  where $x(y,\theta)$ is the set of minimizers of $x \mapsto E(x,y,\theta)$ which is considered nonempty (the minimizer may not be unique but is assumed to exist). The data fidelity term $x \mapsto H(y,\Phi x)$ is defined using a strongly convex map $\mu \mapsto H(y,\mu)$. The regularization term $x \mapsto R(x,\theta)$ is assumed to be a closed proper and convex function, which accounts for the prior structure of x_0. Typical priors correspond to nonsmooth regularizers such as sparsity in a suitable domain, e.g., Fourier, wavelet [46], or gradient [59]. Such regularizers are usually parametrized with a collection of parameters θ. A typical example is $R(x,\theta) = \theta R_0(x)$, where $\theta \in \mathbb{R}^+$ is a scaling which controls the strength of

the regularization. Of course, more complicated (multiparameter) regularizations are often considered in the applications, and our methodology aims at dealing with these higher-dimensional sets of parameters.

An important observation is that even though $x(y,\theta)$ may not be a singleton (the minimizer of $E(x,y,\theta)$ may not be unique), strict convexity of $H(y,\cdot)$ implies that all minimizers share the same image under Φ; see, e.g., [66]. Hence $(y,\theta)\mapsto\mu(y,\theta)$ is defined without ambiguity as a single-valued mapping. Moreover, strong convexity of $H(y,\cdot)$ implies that $y\mapsto\mu(y,\theta)$ is nonexpansive (i.e., uniformly 1-Lipschitz) [67], hence weakly differentiable [29, Theorem 5, section 4.2.3].

- Consider now the ℓth iterate, denoted by $x^{(\ell)}(y,\theta)$, of an iterative algorithm converging to a fixed point of an operator acting on $\mathcal{X}$. In this case, θ can include the parameters of the fixed point operator, as well as other continuous parameters inherent to the fixed point iteration (e.g., step sizes). Section 4 is completely dedicated to this setting, and appropriate sufficient conditions will be exhibited to ensure weak differentiability of $x^{(\ell)}(y,\theta)$ with respect to both its arguments.

  This general setting encompasses the case of proximal splitting methods that have become popular for solving large-scale optimization problems of the form (1.2), especially with convex nonsmooth terms, e.g., those encountered in sparsity regularization. The precise splitting algorithm to be used depends on the structure of the optimization problem at hand. See, for instance, [3, 13] for an overview. Some of these algorithms are considered in detail in section 4.

The choice of θ is generally a challenging task, especially as the dimension of Θ gets large. Ideally, one would like to choose the parameters $\theta^\star$ that make $\mu(y,\theta^\star)$ (or some appropriate image of it) as faithful as possible to μ_0 (or some appropriate image of it). Formally, this can be cast as selecting $\theta^\star$ that minimizes the expected reconstruction error (also known as mean squared error or quadratic risk), i.e.,

$$\theta^\star \in \operatorname*{Argmin}_{\theta\in\Theta} \{R^A\{\mu\}(\mu_0,\theta) = \mathbb{E}_W \|A(\mu(Y,\theta)-\mu_0)\|^2\}, \tag{1.3}$$

where the matrix $A\in R^{M\times P}$ is typically chosen to counterbalance the effect of Φ; see section 2.1 for a precise discussion.

If $\theta\mapsto R^A\{\mu\}(\mu_0,\theta)$ were sufficiently smooth, at least locally (e.g., Lipschitz), one could expect to solve (1.3) using a (sub-)gradient descent scheme relying on the (weak) gradient of the risk $\nabla_2\{R^A\{\mu\}\}(\mu_0,\theta)$, where the subscript 2 specifies that the (weak) gradient is with respect to the second argument θ. However, this would apply only if μ_0 were available. In the context of our observation model (1.1), μ_0 is, however, considered to be unknown. Our motivation then is to build an estimator of $\nabla_2\{R^A\{\mu\}\}(\mu_0,\theta)$ that depends solely on y, without prior knowledge of μ_0.

Toward this goal, we adopt the framework of the (generalized) Stein Unbiased Risk Estimator (SURE) [28, 48, 55, 62, 66]. For a fixed θ, the celebrated Stein lemma [62] allows us to unbiasedly estimate $R^A\{\mu\}(\mu_0,\theta)$ through the weak Jacobian $\partial_1\mu(y,\theta)$, where the subscript 1 specifies that the (weak) Jacobian is with respect to the first argument y. This idea has been exploited for years in several statistical and signal processing applications, typically for selecting thresholds in wavelet-based reconstruction algorithms; see, e.g., [4, 6, 11, 17, 23, 48, 52, 54].

Given such an estimator $\widehat{R}^A\{\mu\}(y,\theta)$ (see section 2.1), the idea is to replace the optimization problem (1.3) with

$$\theta^\star \in \operatorname*{Argmin}_{\theta\in\Theta} \widehat{R}^A\{\mu\}(y,\theta). \tag{1.4}$$

Provided that the variance of $\frac{1}{P}\widehat{R}^A\{\mu\}(Y,\theta)$ can be made arbitrarily small or even asymptotically vanishing as P increases, so that it becomes a consistent estimator of $\frac{1}{P}R^A\{\mu\}(\mu_0,\theta)$, one can expect that the minimizers of (1.4) become close to those of (1.3).

It remains to find an efficient way to solve the optimization (1.4). Again, a (sub-)gradient descent algorithm could qualify as a good candidate if $\theta \mapsto \widehat{R}^A\{\mu\}(y,\theta)$ were sufficiently smooth. To the best of our knowledge, only the authors of [18] have performed such an optimization with Newton's method where $(y,\theta) \mapsto \widehat{R}^A\{\mu\}(y,\theta)$ was C^∞. Unfortunately, being a function of $\partial_1\mu(y,\theta)$, $\theta \mapsto \widehat{R}^A\{\mu\}(y,\theta)$ is in general not differentiable, not even continuous (think of a simple soft-thresholding). This then precludes the use of standard descent schemes.

The common practice has been to apply an exhaustive search by evaluating the risk estimate $\widehat{R}^A\{\mu\}(y,\theta)$ at different values of θ. Even if in some particular cases this can be done efficiently (see, for instance, [23]), the computational expense can become prohibitive in general, especially as $\dim(\Theta)$ increases.

Derivative-free optimization algorithms have also been investigated (see, for instance, [51] for the case of two parameters). However, such approaches typically do not scale up to problems where Θ has a linear vector space structure with dimension larger than 2. Their performance is known to degrade exponentially with problem size, and they require computing a lower and an upper bound on the optimal value over a given region.

Contributions. In this paper, we address the challenging problem of efficiently solving (1.4), a main subject of interest for applications that has been barely investigated. Our main contribution (section 3) is an effective strategy to automatically optimize a collection of parameters θ independently of their dimension. While classical unbiased risk estimates entail optimizing a noncontinuous function of the parameters, we show that the biased risk estimator introduced in [51] is differentiable in the weak sense. This allows us, whenever the derivatives exist, to perform a quasi-Newton optimization driven by a biased estimator of the gradient of the risk based on the evaluation of $\partial_2\mu(y,\theta)$. Such an optimization technique can be provably faster, thanks to first-order information, compared to derivative-free approaches. We prove that, under mild assumptions, this estimator is asymptotically (with respect to P) unbiased, hence the name Stein Unbiased GrAdient estimator of the Risk (SUGAR). Moreover, in the particular case of soft-thresholding, we go a step further and show that it is actually a consistent estimator of the gradient of the risk.

As a second contribution (section 4), we propose a versatile approach to computing the derivatives $\partial_1\mu(y,\theta)$ and $\partial_2\mu(y,\theta)$, involved, respectively, in the computation of the SURE and SUGAR, when $\mu(y,\theta)$ is computed through an iterative algorithm, typically a proximal splitting method. We illustrate the versatility of our method by applying it to both primal algorithms (forward-backward [14], Douglas–Rachford [12], and generalized fowardbackward [50]) and primal-dual algorithms [10] (see [41] for a recent review). The proposed

methodology can, however, be adapted to any other proximal splitting method and more generally to any algorithm whose iteration operator is weakly differentiable.

Numerical simulations involving multiparameter selection for image restoration and matrix completion problems are reported in section 5. The proofs of our results are collected in the appendices.

2. Overview on risk estimation.

This section gives an overview of the literature on estimating the risk via the SURE and its variants for ill-posed inverse problems contaminated by additive white Gaussian noise.

2.1. SURE.

Degrees of freedom (DOF) is often used to quantify the complexity of a statistical modeling procedure; see, for instance, generalized cross-validation [34]. From [27, 66], the DOF of a function $y \mapsto \mu(y,\theta)$ relative to a matrix $A \in R^{M\times P}$ is given by

$$df^A\{\mu\}(\mu_0,\theta) = \sum_{i=1}^{P} \frac{\operatorname{cov}(AY_i, (A\mu(Y,\theta))_i)}{\sigma^2} \tag{2.1}$$

such that $df^A\{\mu\}(\mu_0,\theta)$ is maximal when $A\mu(Y,\theta)$ is highly correlated with the random vector AY. Taking $A = \mathrm{Id}$ leads to the standard definition of the DOF defined in the seminal work of Efron [27]. But other choices of A allow one to counterbalance the undesirable effect of the linear operator Φ (recall that $\mu_0 = \Phi x_0$). For instance, setting $A = (\Phi^*\Phi)^{-1}\Phi^*$ when Φ has full rank, or $A = \Phi^*(\Phi\Phi^*)^+$ when Φ is rank-deficient,[1] provides a measure of the DOF relative to the least-squares estimate of x_0, i.e., $x_{\mathrm{LS}}(y) = Ay$ [28, 48, 66].

With the proviso that $y \mapsto \mu(y,\theta)$ is weakly differentiable with essentially bounded weak partial derivatives, an unbiased estimate of the DOF can be used to unbiasedly estimate the risk in (1.3). This leads to the (generalized) SURE (also known as weighted SURE [53]) given as

$$\begin{aligned} &\mathrm{SURE}^A\{\mu\}(y,\theta) = \|A(\mu(y,\theta)-y)\|^2 - \sigma^2 \operatorname{tr}(A^*A) + 2\sigma^2 \widehat{df}^A\{\mu\}(y,\theta) \\ &\text{with} \quad \widehat{df}^A\{\mu\}(y,\theta) = \operatorname{tr}\left(A\partial_1\mu(y,\theta)A^*\right), \end{aligned} \tag{2.2}$$

where we recall that $\partial_1\mu(y,\theta)$ is the weak Jacobian of $\mu(y,\theta)$ with respect to the first argument y. It can be shown that (see, e.g., [28, 62, 66])

$$\mathbb{E}_W[\widehat{df}^A\{\mu\}(Y,\theta)] = df^A\{\mu\}(\mu_0,\theta) \quad \text{and} \quad \mathbb{E}_W[\mathrm{SURE}^A\{\mu\}(Y,\theta)] = R^A\{\mu\}(\mu_0,\theta).$$

Expression (2.2) is general enough to encompass unbiased estimates of the *prediction* risk $\mathbb{E}_W\|\mu(Y,\theta)-\mu_0\|^2$ (i.e., $A = \mathrm{Id}$), the *projection* risk $\mathbb{E}_W\|\Pi(x(Y,\theta)-x_0)\|^2$, where Π is the orthogonal projector on $\ker(\Phi)^\perp$ (i.e., $A = \Phi^*(\Phi\Phi^*)^+$), and the *estimation* risk $\mathbb{E}_W\|x(Y,\theta)-x_0\|^2$ when Φ has full rank (i.e., $A = (\Phi^*\Phi)^{-1}\Phi^*$). This can prove useful when Φ is rank-deficient, since, in this case, the minimizers of the prediction risk can be far away from the minimizers of the estimation risk [56]. The projection risk restricts the estimate to the subspace where there is a signal in addition to noise, and in this sense, is a good approximation of the estimation risk [28].

[1] $(\cdot)^+$ stands for the Moore–Penrose pseudoinverse.

Note that generalization of the SURE have been developed for other noise models, typically within the multivariate canonical exponential family (see, e.g., [28, 37, 38, 55]).

Applications of the SURE emerged for choosing the smoothing parameters in families of linear estimates [44], such as model selection, ridge regression, and smoothing splines. After its introduction in the wavelet community with the SURE-Shrink algorithm [23], the SURE has been widely used for various image restoration problems, e.g., with sparse regularizations [4, 6, 7, 11, 17, 45, 48, 51, 52, 53, 54, 70] or with nonlocal filters [16, 25, 68, 69].

However, a major practical difficulty when using the SURE lies in the numerical computation of the DOF estimate, i.e., the quantity $\widehat{df}^{A}\{\mu\}(y,\theta)$ for a given realization y. We now give a brief overview of some previous work to deal with this computation.

2.2. Closed-form SURE. The SURE is based on a DOF estimate $\widehat{df}^{A}\{\mu\}(Y,\theta)$ that can be sampled from the observation $y \in \mathbb{R}^P$ by evaluating the Jacobian $\partial_1\mu(y,\theta) \in \mathbb{R}^{N\times P}$. A natural way to evaluate $\partial_1\mu(y,\theta)$ would be to derive its closed-form expression. This has been studied for some classes of variational problems.

In quadratic regularization (e.g., ridge regression), where solutions are of the form $x(y,\theta) = K(\theta)y$, where $K(\theta)$ is known as the hat or influence matrix, the Jacobian has a closed-form $\partial_1\mu(y,\theta) = \Phi K(\theta)$. In ℓ^1-synthesis regularization (also known as the lasso), the Jacobian matrix depends on the support (set of nonzero coefficients) of any lasso solution $x(y,\theta)$. An estimator of the DOF can then be retrieved from the number of nonzero entries of this solution [24, 65, 73]. These results have in turn been extended to more general sparsity promoting regularizations [21, 40, 61, 64, 65, 66, 72] and spectral regularizations (e.g., nuclear norm) [9, 20].

This approach, however, has three major bottlenecks. First, deriving the closed-form expression of the Jacobian is, in general, challenging and has to be addressed on a case-by-case basis. Second, in large-dimensional problems, evaluating this Jacobian numerically is barely possible. Even if it were possible, it might be subject to serious numerical instabilities. Indeed, solutions of variational problems are achieved via iterative schemes providing iterates $x^{(\ell)}(y,\theta)$ that eventually converge to the set of solutions as $\ell \to +\infty$. And yet, for instance, substituting the support of the true solution by the support of $x^{(\ell)}(y,\theta)$, obtained at a prescribed convergence accuracy, might be imprecise (all the more since the problem is ill-conditioned).

The next three sections review previous work to address one or more of these three points.

2.3. Monte-Carlo SURE. To deal with the large dimension of the Jacobian, the standard approach is to exploit the fact that the DOF depends only on the trace of $A\partial_1\mu(y,\theta)A^*$. In denoising applications where $A = \mathrm{Id}$ and $\Phi = \mathrm{Id}$, this trace can generally be obtained by closed-form computations of the P diagonal elements of $\partial_1\mu(y,\theta)$ (see, e.g., [23, 68]). This can also be done for some particular inverse problems. For instance, the authors of [48] provide an expression of this trace for the wavelet-vaguelette estimator when Φ is a convolution matrix and $A = \Phi^+$. However, in more general settings, the complexity of the closed-form computation of the trace is nonlinear; typically the number of operations is in $O(P\times P)$ (think of Φ as a mixing operator or μ as an iterative estimator). To avoid such a costly procedure, the authors of [32, 51] suggest making use of the following trace equality:

$$\widehat{df}^{A}\{\mu\}(y,\theta) = \mathrm{tr}\left(A\partial_1\mu(y,\theta)A^*\right) = \mathbb{E}_\Delta\left\langle \partial_1\mu(y,\theta)[\Delta],\, A^*A\Delta\right\rangle, \tag{2.3}$$

where $\Delta \sim \mathcal{N}(0, \mathrm{Id}_P)$ and $\partial_1 \mu(y,\theta)[\delta] \in \mathbb{R}^P$ denotes the directional derivative of $y \mapsto \mu(y,\theta)$ at y in direction δ. Remark that Δ does not necessarily have to be Gaussian and higher precisions can be reached in some specific cases; see, for instance, [2, 22, 39, 58]. As shown in [58], the performance of this trace estimator is governed by the distribution of the singular values of the operator $A\partial_1\mu(y,\theta)A^*$. More specifically, the slower the decay, the better the performance. While it is difficult to make a general claim, we observed numerically that for the recovery problems we consider, it provide a very accurate estimator of the trace. Hence, following [51, 70], an estimate of $\mathrm{SURE}^A\{\mu\}(y,\theta)$ can be obtained by Monte-Carlo simulations using

$$\begin{aligned} &\mathrm{SURE}^A_{\mathrm{MC}}\{\mu\}(y,\theta,\delta) = \|A(\mu(y,\theta)-y)\|^2 - \sigma^2 \operatorname{tr}(A^*A) + 2\sigma^2 \widehat{df}^A_{\mathrm{MC}}\{\mu\}(y,\theta,\delta) \\ &\text{with} \quad \widehat{df}^A_{\mathrm{MC}}\{\mu\}(y,\theta,\delta) = \langle \partial_1\mu(y,\theta)[\delta],\, A^*A\delta \rangle. \end{aligned} \tag{2.4}$$

The evaluation of (2.4) necessitates only computing the P entries of $\partial_1\mu(y,\theta)[\delta]$.

It remains to find a stable and efficient way to evaluate for any vector $\delta \in \mathbb{R}^P$ the directional derivative $\partial_1\mu(y,\theta)[\delta] \in \mathbb{R}^P$.

2.4. Iterative differentiation for Monte-Carlo SURE. When considering solutions $x(y,\theta)$ of a variational problem, the DOF cannot be robustly estimated if one knows only the iterates $\mu^{(\ell)}(y,\theta)$ that eventually converge to some $\mu(y,\theta)$ as $\ell \to +\infty$. It then appears natural to estimate the DOF of $\mu^{(\ell)}(Y,\theta)$ directly and make the assumption that it will converge to that of $\mu(y,\theta)$. For a realization $y \in \mathbb{R}^P$, one can sample an estimate of the DOF of the iterate $\mu^{(\ell)}(Y,\theta)$ by evaluating its directional derivative $\partial_1\mu^{(\ell)}(y,\theta)[\delta]$. A practical way, initiated by [70], to compute this quantity consists in recursively differentiating the sequence of iterates. The authors of [70] have derived the closed-form expression of the directional derivative for the forward-backward (FB) algorithm. The directional derivative at iteration $\ell+1$, denoted by $\mathcal{D}_\mu^{(\ell+1)} = \partial_1\mu^{(\ell+1)}(y,\theta)[\delta]$, is obtained iteratively as a function of $\mu^{(\ell)}(y,\theta)$ and $\mathcal{D}_\mu^{(\ell)} = \partial_1\mu^{(\ell)}(y,\theta)[\delta]$. The Monte-Carlo DOF and the Monte-Carlo SURE can in turn be iteratively estimated by plugging $\partial_1\mu^{(\ell)}(y,\theta)[\delta]$ into (2.4), leading to

$$\begin{aligned} &\mathrm{SURE}^A_{\mathrm{MC}}\{\mu^{(\ell)}\}(y,\theta,\delta) = \left\|A(\mu^{(\ell)}(y,\theta)-y)\right\|^2 - \sigma^2 \operatorname{tr}(A^*A) + 2\sigma^2 \widehat{df}^A_{\mathrm{MC}}\{\mu^{(\ell)}\}(y,\theta,\delta) \\ &\text{with} \quad \widehat{df}^A_{\mathrm{MC}}\{\mu^{(\ell)}\}(y,\theta,\delta) = \left\langle \mathcal{D}_\mu^{(\ell)},\, A^*A\delta \right\rangle. \end{aligned} \tag{2.5}$$

A similar approach is described in [33]. Pursuing this idea, the authors of [52, 53] recently provided such closed-form expressions in the case of the split Bregman method. Concurrently, in an early short version of this paper [19], we have also considered this approach for general proximal splitting algorithms, an approach that we extend in section 4.

2.5. Finite-difference SURE. An alternative initiated in [60, 71] and rediscovered in [51] consists in estimating $\operatorname{tr}(A\partial_1\mu(y,\theta)A^*)$ via finite differences given, for $\varepsilon > 0$, by

$$\operatorname{tr}(A\partial_1\mu(y,\theta)A^*) \approx \sum_{i=1}^{P} \frac{[A^*A(\mu(y+\varepsilon e_i,\theta)-\mu(y,\theta))]_i}{\varepsilon}, \tag{2.6}$$

where $(e_i)_{1\leqslant i\leqslant P}$ is the canonical basis of $\mathbb{R}^P$. Plugging this expression into (2.4) yields the finite-difference (FD) SURE^A given by

$$\mathrm{SURE}^A_{\mathrm{FD}}\{\mu\}(y,\theta,\varepsilon) = \|A(\mu(y,\theta)-y)\|^2 - \sigma^2\operatorname{tr}(A^*A) + 2\sigma^2\widehat{df}^A_{\mathrm{FD}}\{\mu\}(y,\theta,\varepsilon)$$

$$\text{with}\quad \widehat{df}^A_{\mathrm{FD}}\{\mu\}(y,\theta,\varepsilon) = \frac{1}{\varepsilon}\sum_{i=1}^{P}(A^*A(\mu(y+\varepsilon e_i,\theta)-\mu(y,\theta)))_i. \tag{2.7}$$

The main advantage of this method is that $(y,\theta)\mapsto\mu(y,\theta)$ can be used as a black box, i.e., without knowledge of the underlying algorithm that provides $\mu(y,\theta)$, while, for ε small enough, it performs as well as the approach described in section 2.4 that requires the knowledge of the derivatives in closed form. In fact, if $y\mapsto\mu(y,\theta)$ is Lipschitz-continuous, then it is differentiable Lebesgue-a.e. (Rademacher's theorem), and its derivative equals its weak derivative Lebesgue-a.e. [29, Theorems 1–2, section 6.2], which in turn implies

$$\lim_{\varepsilon\to 0}\mathrm{SURE}^A_{\mathrm{FD}}\{\mu\}(y,\theta,\varepsilon) = \mathrm{SURE}^A\{\mu\}(y,\theta)\quad\text{Lebesgue-a.e.} \tag{2.8}$$

The value of ε can thus be chosen as small as possible as soon as it does not rise to numerical instabilities due to limited machine precision. To avoid numerical instabilities, ε should be chosen in a reasonable range of values with respect to the amplitudes of the data. In practice, we observe that for such choices of ε, accurate results can be reached, very close to the closed-form derivation, hence yielding to a quasi-unbiased risk estimator (i.e., with a negligible bias). It remains that when the data dimension P is large, the evaluation of P finite differences along each axis might be numerically intractable. In that case, the Monte-Carlo approach (see section 2.3) can also be used in conjunction with finite differences leading to the finite-difference Monte-Carlo (FDMC) SURE^A given by

$$\mathrm{SURE}^A_{\mathrm{FDMC}}\{\mu\}(y,\theta,\delta,\varepsilon) = \|A(\mu(y,\theta)-y)\|^2 - \sigma^2\operatorname{tr}(A^*A) + 2\sigma^2\widehat{df}^A_{\mathrm{FDMC}}\{\mu\}(y,\theta,\delta,\varepsilon)$$

$$\text{with}\quad \widehat{df}^A_{\mathrm{FDMC}}\{\mu\}(y,\theta,\delta,\varepsilon) = \frac{1}{\varepsilon}\left\langle\mu(y+\varepsilon\delta,\theta)-\mu(y,\theta),\, A^*A\delta\right\rangle. \tag{2.9}$$

The originality of our approach described in the next section is to devise a grounded choice of $\varepsilon>0$. This introduces a bias in the estimation of the risk. Nevertheless, as we will see, using $\varepsilon>0$ plays an important role in risk optimization since, unlike $\mathrm{SURE}^A\{\mu\}$, $\mathrm{SURE}^A_{\mathrm{FD}}\{\mu\}$ is a smooth function of θ in the weak sense. This is the key point in optimizing the risk. By choosing $\varepsilon>0$ carefully, a smoother objective function can be used as a basis to perform a quasi-Newton–like optimization at the expense of a controlled bias.

3. Risk estimate minimization.

In this section, we investigate how risk estimates can be used for optimizing a collection of continuous parameters.

3.1. SUGAR.

The difficulty is that even if $\theta\mapsto R^A\{\mu\}(\mu_0,\theta)$ is differentiable in the weak sense, the function $\theta\mapsto\mathrm{SURE}^A\{\mu\}(y,\theta)$ might contain discontinuities. Typically, $\widehat{df}^A\{\mu\}(y,\theta)$ has discontinuities where $(y,\theta)\mapsto\mu(y,\theta)$ is not differentiable.

We start with a simple result showing that, unlike $\mathrm{SURE}^A\{\mu\}(y,\theta)$, the finite-difference–based mapping $\theta \mapsto \mathrm{SURE}^A_{\mathrm{FD}}\{\mu\}(y,\theta,\varepsilon)$, for $\varepsilon > 0$, is weakly differentiable.

Proposition 1. *Assume $\mu(y,\theta)$ is weakly differentiable with respect to y and θ. Given $\varepsilon > 0$, $\widehat{df}^A_{\mathrm{FD}}\{\mu\}(y,\theta,\varepsilon)$ and $\mathrm{SURE}^A_{\mathrm{FD}}\{\mu\}(y,\theta,\varepsilon)$ are also weakly differentiable with respect to y and θ, and their (weak) gradients with respect to θ are given, for almost all $\theta \in \Theta$, as*

$$\begin{aligned}
\mathrm{SUGAR}^A_{\mathrm{FD}}\{\mu\}(y,\theta,\varepsilon) &= \nabla_2\{\mathrm{SURE}^A_{\mathrm{FD}}\{\mu\}\}(y,\theta,\varepsilon) \\
&= 2\partial_2\mu(y,\theta)^* A^* A(\mu(y,\theta)-y) + 2\sigma^2 \nabla_2\{\widehat{df}^A_{\mathrm{FD}}\{\mu\}\}(y,\theta,\varepsilon), \\
\textit{where}\quad \nabla_2\{\widehat{df}^A_{\mathrm{FD}}\{\mu\}\}(y,\theta,\varepsilon) &= \frac{1}{\varepsilon}\sum_{i=1}^{P} (\partial_2\mu(y+\varepsilon e_i,\theta) - \partial_2\mu(y,\theta))^* A^* A e_i.
\end{aligned}$$

Thanks to Proposition 1, a quasi-Newton–like method can now be used to optimize $\mathrm{SURE}^A_{\mathrm{FD}}\{\mu\}(y,\theta,\varepsilon)$ for the vector of continuous parameters θ by implementing the iteration

$$\theta_{n+1} = \theta_n - B_n \mathrm{SUGAR}^A_{\mathrm{FD}}\{\mu\}(y,\theta_n,\varepsilon),$$

where $B_n \in \mathbb{R}^{\dim(\Theta)\times\dim(\Theta)}$ is a sequence of definite-positive matrices. Typically, if $\theta \mapsto \mathrm{SURE}^A_{\mathrm{FD}}\{\mu\}(y,\theta,\delta,\varepsilon)$ behaves locally as a C^2 function, B_n should approach the inverse of the corresponding Hessian at θ_n. Remark that in general there is no guarantee that the risk has a unique global minimizer, though in the one-dimensional case it is generally the case. When several parameters are involved, such an objective can have several local minima and specific quasi-Newton–like methods might be developed to avoid being stuck in one of them.

In practice, the calculation of $\mathrm{SUGAR}^A_{\mathrm{FD}}$ depends on the computation of the Jacobian matrices with respect to the parameters θ. We will see in section 4 how this quantity can be efficiently computed when μ results from an iterative algorithm.

We now turn to the asymptotic unbiasedness of the proposed gradient estimator of the risk as ε approaches 0. Toward this goal we need the following assumptions.

(A1) The mapping $y \mapsto \mu(y,\theta)$ is uniformly Lipschitz continuous with Lipschitz constant L_1.

(A2) The mapping $y \mapsto \mu(y,\theta)$ is such that $\mu(0,\theta) = 0$ for any θ.

(A3) The mapping $\theta \mapsto \mu(y,\theta)$ is uniformly Lipschitz continuous with Lipschitz constant L_2 independently of y.

Remark 1 (discussion of the assumptions).

1. Assumption (A1) is mild and is fulfilled in many situations of interest. In particular, this is the case when $y \mapsto \mu(y,\theta) = \mathrm{Prox}_{\theta F}(y)$, $\theta > 0$, is the proximal operator of a proper closed and convex function F, as considered in section 4 (see also section 3.2 for soft-thresholding). Standard convex analysis arguments [36] show that the proximal operator is indeed a uniformly Lipschitz mapping of its argument y with constant $L_1 = 1$, independently of θ.
2. Assumption (A2) is very natural and does not entail any loss of generality. It basically states that, when the observations are zero, so is the estimator.
3. As far as assumption (A3) is concerned, it is verified under certain circumstances. This is, for instance, the case when $\mu(y,\theta) = \mathrm{Prox}_{\theta G}(y)$, $\theta > 0$, where G is the gauge (see Definition 2 in Appendix B) of any compact convex set containing the origin as an

interior point;[2] see Proposition 5 in Appendix B. By induction, this also holds when $\mu(y,\theta) = \mathrm{Prox}_{\theta_1 G_1} \circ \cdots \circ \mathrm{Prox}_{\theta_m G_m}(y)$, $\theta \in]0,+\infty[^m$, and for any $i = 1,\dots,m$, G_i is the gauge of any compact convex set containing the origin as an interior point; see Corollary 5. Typical instances of these gauges are norms, e.g., ℓ_1, $\ell_1 - \ell_2$, or nuclear norms now very popular in the signal and image processing community.

4. Assumption (A3) can be relaxed to cover the case where L_2 depends on y. In such a situation, additional assumptions on the function $y \mapsto L_2(y)$ are needed for steps (S.3) and (S.4) in the proof of Theorem 1 to proceed. We omit this case for the sake of clarity and to avoid further technicalities.

We are now ready to state our theorem.

Theorem 1 (asymptotic unbiasedness of SUGAR). *Assume that assumptions (A1)–(A3) hold. Then, $R^A\{\mu\}(\mu_0,\cdot)$ and $df^A\{\mu\}(\mu_0,\cdot)$ are weakly differentiable, and for any Lebesgue point θ,*

$$\lim_{\varepsilon\to 0} \mathbb{E}_W\left[\mathrm{SUGAR}^A_{\mathrm{FD}}\{\mu\}(Y,\theta,\varepsilon)\right] = \nabla_2\{R^A\{\mu\}\}(\mu_0,\theta),$$
$$\lim_{\varepsilon\to 0} \mathbb{E}_W\left[\nabla_2\{\widehat{df}^A_{\mathrm{FD}}\{\mu\}\}(Y,\theta,\varepsilon)\right] = \nabla_2\{df^A\{\mu\}\}(\mu_0,\theta).$$

Theorem 1 can be given the following interpretation. As ε gets close to 0, e.g., a decreasing function of the dimension P,[3] the gradient of $\mathrm{SURE}^A_{\mathrm{FD}}\{\mu\}(y,\cdot,\varepsilon)$ (normalized by P) can be used to estimate the gradient of the risk (also normalized by P), provided that P is large enough.

However, even if ε should decrease toward 0, it should not decrease too fast. In particular, for a fixed dimension P, the step ε cannot be chosen arbitrarily small. This would not be an issue if $\mu(y,\cdot)$ were differentiable, but, in general, there might be singularities. In fact, for a finite dimension P, the limit when $\varepsilon \to 0$ of the sample $\mathrm{SUGAR}^A_{\mathrm{FD}}\{\mu\}(y,\theta,\varepsilon)$ may not even exist, though that of its expectation does exist Lebesgue-a.e., as shown in the proof of Theorem 1. As a consequence, the quantity $\frac{1}{P}\mathrm{SUGAR}^A_{\mathrm{FD}}\{\mu\}(Y,\theta,\varepsilon)$ can become very unstable when ε decreases too quickly with the dimension P. The underlying statistical question is whether one can control the variance of $\frac{1}{P}\mathrm{SUGAR}^A_{\mathrm{FD}}\{\mu\}(Y,\theta,\varepsilon)$ as P increases, and make it arbitrarily small or even asymptotically vanishing, so that $\frac{1}{P}\mathrm{SUGAR}^A_{\mathrm{FD}}\{\mu\}(Y,\theta,\varepsilon)$ becomes a consistent estimator. Unfortunately, consistency of our gradient estimator of the risk is very intricate to get in the general case, as is the case for the consistency of the SURE. However, when μ specializes to soft-thresholding, such a result can be achieved.

3.2. SUGAR for soft-tresholding.

In this section, we show that the proposed gradient estimator of the risk can be consistent in the case where μ is the soft-thresholding (ST) function and $A = \mathrm{Id}_P$. The soft-thresholding is the proximal operator of the ℓ_1-norm. Understanding the soft-thresholding is of chief interest since it is at the heart of any proximal splitting algorithm solving a regularized inverse problem involving terms of the form $\|D^* x\|_1$, where D is a linear operator.

Let us first recall the definition of soft-thresholding.

[2] Another case which is trivial corresponds to G being the indicator function of a nonempty closed convex set, in which case $L_2 = 0$.

[3] As we will see, the higher the dimension P is, the smaller ε can be.

Definition 1 (soft-thresholding). *The soft-thresholding (ST) is defined, for $\lambda > 0$ and for all $1 \leqslant i \leqslant P$, as*

$$\mathrm{ST}(y,\lambda)_i = \begin{cases} y_i + \lambda & \text{if} \quad y_i \leqslant -\lambda, \\ 0 & \text{if} \quad -\lambda < y_i < \lambda, \\ y_i - \lambda & \text{otherwise.} \end{cases} \tag{3.1}$$

Observe that as a proximal operator of a norm, soft-thresholding satisfies assumptions (A1)–(A3) of Theorem 1; see the corresponding discussion. Hence, we already anticipate from Theorem 1 that our gradient estimator of the soft-thresholding risk is asymptotically unbiased.

We start with following lemma which collects the statistics of the gradient of the finite-difference DOF estimator.

Lemma 1 (statistics of the gradient of the finite-difference DOF estimator). *Let $0 < \varepsilon < 2\lambda$. The weak gradient of $\lambda \mapsto \widehat{df}_{\mathrm{FD}}\{\mathrm{ST}\}(Y,\lambda,\varepsilon)$ is such that*

$$\mathbb{E}_W\left[\nabla_2\{\widehat{df}_{\mathrm{FD}}\{\mathrm{ST}\}\}(Y,\lambda,\varepsilon)\right] = \frac{-1}{2}\sum_{i=1}^{P}\frac{\varphi[(\mu_0)_i,\lambda,\varepsilon]}{\varepsilon},$$
$$\mathbb{V}_W\left[\nabla_2\{\widehat{df}_{\mathrm{FD}}\{\mathrm{ST}\}\}(Y,\lambda,\varepsilon)\right] = \frac{1}{2\varepsilon}\sum_{i=1}^{P}\frac{\varphi[(\mu_0)_i,\lambda,\varepsilon]}{\varepsilon} - \frac{1}{4}\sum_{i=1}^{P}\left[\frac{\varphi[(\mu_0)_i,\lambda,\varepsilon]}{\varepsilon}\right]^2,$$

where for $a \in \mathbb{R}$, $\varphi[a,\lambda,\varepsilon] = \mathrm{erf}(\frac{a+\lambda+\varepsilon}{\sqrt{2}\sigma}) - \mathrm{erf}(\frac{a+\lambda}{\sqrt{2}\sigma}) + \mathrm{erf}(\frac{a-\lambda+\varepsilon}{\sqrt{2}\sigma}) - \mathrm{erf}(\frac{a-\lambda}{\sqrt{2}\sigma})$.

We now turn to the asymptotic behavior of the proposed gradient estimator of the risk for large P at a single realization of Y, i.e., our observation y. To this end, we first have to define how the observation model evolves with the dimension P. Given $z_0 \in \mathbb{R}^N$, we consider the sequence $\{\Psi_P\}_{P\geqslant 1}$, where, for all $P \geq 1$, $\Psi_P \in \mathbb{R}^{P\times N}$ is the submatrix obtained by deleting one line of Ψ_{P+1}. We can then define a sequence of observation models as the sequence of random vector $\{Y_P\}_{P\geqslant 1}$ defined as

$$Y_P = \Psi_P z_0 + W_P, \quad \text{where} \quad W_P \sim \mathcal{N}(0,\sigma^2\mathrm{Id}_P). \tag{3.2}$$

We also define the sequence $\{(\mu_0)_P\}_{P\geqslant 1}$, where $(\mu_0)_P = \Psi_P z_0$. In the following, for the sake of clarity, we omit the dependency of Y_P, W_P, and $(\mu_0)_P$ on P.

We can now state our consistency result for soft-thresholding.

Theorem 2 (consistency of SUGAR). *Take a function $\hat{\varepsilon}(P)$ such that $\lim_{P\to\infty}\hat{\varepsilon}(P) = 0$ and $\lim_{P\to\infty} P^{-1}\hat{\varepsilon}(P)^{-1} = 0$. Then for any Lebesgue point $\lambda > 0$ (i.e., such that, for all (i,P), $\lambda \neq |Y_i|$ and $\lambda \neq |Y_i + \hat{\varepsilon}(P)e_i|$),*

$$\operatorname*{plim}_{P\to\infty}\left[\frac{1}{P}\left(\mathrm{SUGAR}_{\mathrm{FD}}\{\mathrm{ST}\}(Y,\lambda,\hat{\varepsilon}(P)) - \nabla_2\{R\{\mathrm{ST}\}\}(\mu_0,\lambda)\right)\right] = 0,$$
$$\operatorname*{plim}_{P\to\infty}\left[\frac{1}{P}\left(\nabla_2\{\widehat{df}_{\mathrm{FD}}\{\mathrm{ST}\}\}(Y,\lambda,\hat{\varepsilon}(P)) - \nabla_2\{df\{\mathrm{ST}\}\}(\mu_0,\lambda)\right)\right] = 0.$$

In plain words, Theorem 2 asserts that for our gradient estimator of the soft-thresholding risk to be consistent, $\hat{\varepsilon}(P)$ should not decrease faster than the inverse of the dimension P. With

the proviso that $\hat{\varepsilon}(P)$ fulfills the requirement, for P large enough, $\frac{1}{P}\mathrm{SUGAR}_{\mathrm{FD}}\{\mathrm{ST}\}(y,\lambda,\hat{\varepsilon}(P))$ is guaranteed to come close to $\frac{1}{P}\nabla_2\{R\{\mathrm{ST}\}\}(\mu_0,\lambda)$ with high probability.

Unfortunately, Theorem 2 does not dictate an explicit choice of $\hat{\varepsilon}(P)$, and the practitioner may wonder how to choose this value for a given P. It turns out that studying the mean squared error (MSE) of the gradient of the finite-difference DOF estimator helps in unveiling the link between P and ε through a bias-variance trade-off.

Proposition 2 (MSE of the gradient of the finite-difference DOF estimator). *The weak gradient of* $\lambda \mapsto \widehat{df}\{\mathrm{ST}\}(Y,\lambda,\varepsilon)$ *is such that*

$$\mathbb{E}_W\left[\frac{1}{P}\left(\nabla_2\{\widehat{df}\{\mathrm{ST}\}\}(Y,\lambda,\varepsilon)-\nabla_2\{df\{\mathrm{ST}\}\}(\mu_0,\lambda)\right)\right]^2$$
$$=\underbrace{\frac{1}{P^2}\left(\mathbb{E}_W\left[\nabla_2\{\widehat{df}\{\mathrm{ST}\}\}(Y,\lambda,\varepsilon)\right]-\nabla_2\{df\{\mathrm{ST}\}\}(\mu_0,\lambda)\right)^2}_{Bias^2}+\underbrace{\frac{1}{P^2}\mathbb{V}_W\left[\nabla_2\{\widehat{df}\{\mathrm{ST}\}\}(Y,\lambda,\varepsilon)\right]}_{Variance},$$

where the statistics of $\nabla_2\{\widehat{df}\{\mathrm{ST}\}\}(Y,\lambda,\varepsilon)$ *are given in Lemma 1 and*

$$\nabla_2\{df\{\mathrm{ST}\}\}(\mu_0,\lambda)=\frac{-1}{\sqrt{2\pi}\sigma}\sum_{i=0}^{P}\left[\exp\left(-\frac{((\mu_0)_i+\lambda)^2}{2\sigma^2}\right)+\exp\left(-\frac{((\mu_0)_i-\lambda)^2}{2\sigma^2}\right)\right].$$

Thus, if μ_0 were given, the quantities in Proposition 2 could be computed in closed form. The MSE can then be evaluated to select the optimal value of ε for a fixed dimension P and a given threshold λ. The following numerical experiments, detailed hereafter and illustrated in Figure 1, highlight this relationship. When μ_0 is unknown, an a priori model can be imposed, such as, for instance, belonging to some ball promoting sparsity, e.g., a weak ℓ_γ-ball for $\gamma>0$. For γ sufficiently small, this ball corresponds to compressible or nearly sparse vectors μ_0 whose entries $|\mu_i|$ sorted in descending order of magnitude behave as $O(i^{-1/\gamma})$. With such a model at hand, the MSE in Proposition 2 can be optimized for ε given P, σ, λ, and γ. This, however, entails a highly nonlinear equation that cannot be solved in closed form. We defer such a development to a future work.

Figure 1(a) shows the evolution of the bias and the variance as a function of the ratio ε/σ for fixed values of σ, λ, and a compressible vector μ_0, i.e., $|(\mu_0)_i|=O(i^{-1/\gamma})$, chosen as illustrated in Figure 1(d). When $\varepsilon\to 0$, for fixed P, the bias vanishes, while the variance, and, in turn, the MSE, increase. However, for a step $\varepsilon>0$, the MSE is finite and seems to be optimal around the value 0.1σ. Figure 1(c) shows the evolution of the MSE as a function of the dimension P and the ratio ε/σ for the same fixed values as before. The optimal step, minimizing the MSE, seems to evolve as a power decay function (the scale is log-log) of the form $\varepsilon^\star(P)=C\sigma/P^\alpha$ with $C>0$ and $0<\alpha<1$. Of course the optimal constants C and α depend on the choice of μ_0, σ, and λ. However, for any $C>0$ and $0<\alpha<1$, or, more generally, for any admissible choice of $\hat{\varepsilon}$ such that $\lim_{P\to\infty}\hat{\varepsilon}(P)=0$ and $\lim_{P\to\infty}P^{-1}\hat{\varepsilon}(P)^{-1}=0$, the MSE vanishes with respect to P. Figure 1(b) shows indeed the evolution of the bias, the variance, and the MSE as a function of the dimension P when $\hat{\varepsilon}$ is chosen as a power decay function. For $\alpha=0$ or $\alpha=1$, the MSE remains constant, while, for $\alpha>1$, the MSE diverges, which suggests the necessity of $\lim_{P\to\infty}P^{-1}\hat{\varepsilon}(P)^{-1}=0$.

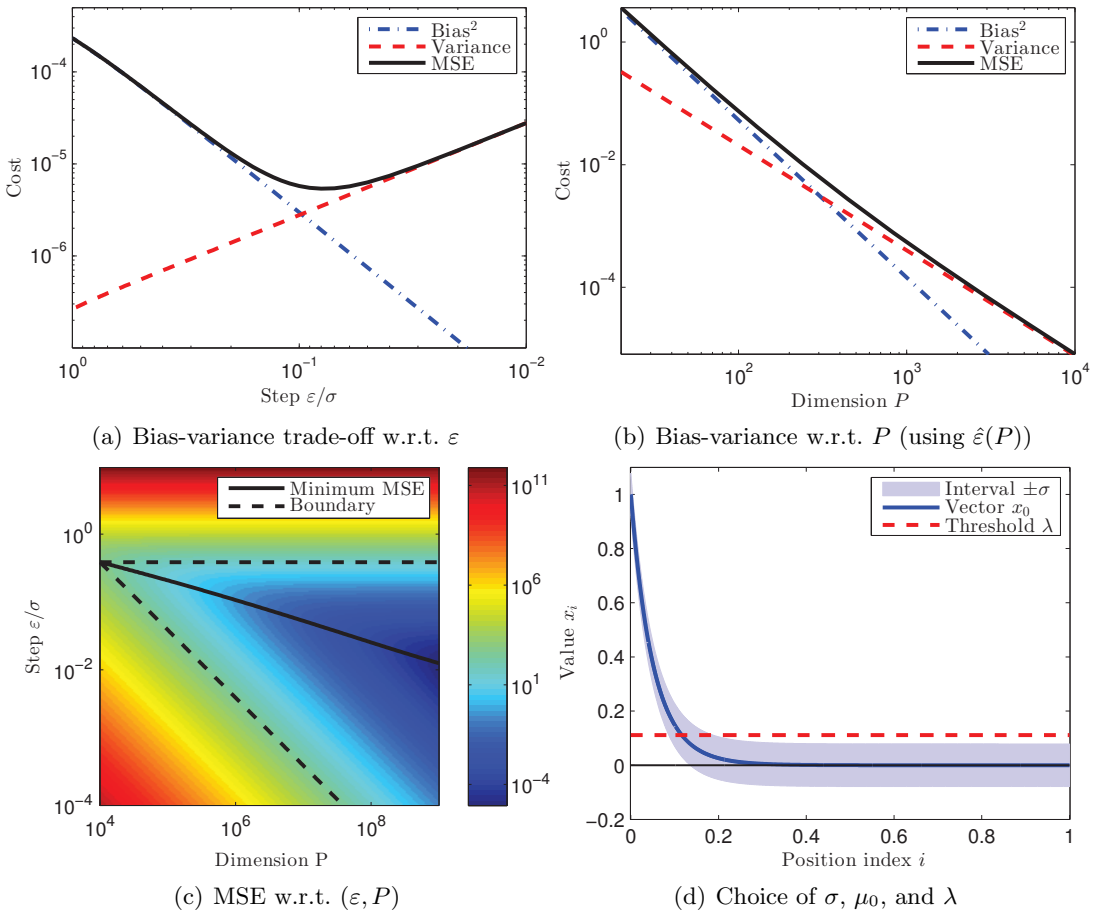

(a) Bias-variance trade-off w.r.t. ε

(b) Bias-variance w.r.t. P (using $\hat{\varepsilon}(P)$)

(c) MSE w.r.t. (ε, P)

(d) Choice of σ, μ_0, and λ

Figure 1. *Bias-variance trade-off of the gradient estimator of the DOF of soft-thresholding,* (a) *with respect to the step* ε*, and* (b) *with respect to the dimension* P *when using a power decay function* $P \mapsto \hat{\varepsilon}(P)$*.* (c) *Its MSE as a function of* P *and* ε *(in logarithmic scales). The solid line represents the pairs* $(\hat{\varepsilon}^\star(P), P)$*, where, for a fixed dimension* P*,* $\hat{\varepsilon}^\star(P)$ *minimizes the MSE. The function* $\hat{\varepsilon}^\star(P)$ *looks like a power function of the form* $C\sigma/P^\alpha$ *with* $C > 0$ *and* $0 < \alpha < 1$*. The dashed lines represent the power functions* $\hat{\varepsilon}^{\inf}(P) = C\sigma$ *and* $\hat{\varepsilon}^{\sup}(P) = C\sigma/P$ *outside of which the MSE diverges when* P *increases.* (d) *Description of the settings of the experiments, i.e., the choice of* σ*,* μ_0*, and* λ*.*

4. Differentiation of an iterative scheme.

We now turn to iterative algorithms that involve linear and soft-thresholding operators. We observed empirically that for all the inverse problems exposed in section 5, setting $\varepsilon^\star(P) = C\sigma/P^\alpha$, as suggested by our study on the soft-thresholding, resulted in a reliable way to parametrize our estimator. The effectiveness of this heuristic might be explained by the fact that the singularities encountered in most imaging problems are similar to absolute values, in order to encourage some sort of sparsity in the solution.

In this section, we focus on iterates, defined unambiguously as single-valued mappings $(y, \theta) \mapsto x^{(\ell)}(y, \theta)$, where ℓ is the iteration counter of the iterative algorithm. In this context, we propose to compute in closed form the derivatives of $x^{(\ell)}(y, \theta)$ with respect to either y (in a direction δ) or θ. This proves useful in estimating, respectively, the risk via $\mathrm{SURE}^A_{\mathrm{MC}}$ (see

section 2) and its gradient via $\mathrm{SUGAR}^{A}_{\mathrm{FDMC}}$ (see section 3).

The iterative schemes we consider can be cast in the same framework, which subsumes proximal splitting algorithms designed to minimize a proper, closed, and convex objective function $x \mapsto E(x, y, \theta)$, whose set of minimizers is supposed nonempty. All these algorithms can be unified as an iterative scheme of the form

$$\begin{cases} x^{(\ell)} & = \gamma(a^{(\ell)}), \\ a^{(\ell+1)} & = \psi(a^{(\ell)}, y, \theta), \end{cases} \tag{4.1}$$

where $a^{(\ell)} \in \mathcal{A}$ is a sequence of auxiliary variables. $\psi : \mathcal{A} \times \mathcal{Y} \times \Theta \to \mathcal{A}$ is a fixed point operator such that $a^{(\ell)}$ converge to a fixed point $a^\star$, and $\gamma : \mathcal{A} \to \mathcal{X}$ is nonexpansive (i.e, $\|\gamma(a_1) - \gamma(a_2)\| \leqslant \|a_1 - a_2\|$ for any $a_1, a_2 \in \mathcal{A}$), entailing that $x^{(\ell)}$ will converge to $x^\star = \gamma(a^\star)$. Note that for the sake of clarity, we have dropped the dependencies of $a^\star$ and $x^\star$ on y and θ.

To make our ideas clear, consider the instructive example where $x \mapsto E(x, y, \theta)$ is convex and $C^1(\mathcal{X})$ with L-Lipschitz gradient, in which case $\mathcal{A} = \mathcal{X}$, $a = x$, and $\psi(x, y, \theta) = x - \tau \nabla_1 E(x, y, \theta)$, where $0 < \tau < 2/L$.

4.1. Iterative weak differentiability. A practical way to get the weak directional derivative $\partial_1 x(y, \theta)[\delta]$ and the weak Jacobian $\partial_2 x(y, \theta)$ is to compute them iteratively from the sequences (4.1) by relying on the chain rule. However, two major issues have to be taken care of. First, one has to ensure weak differentiability of the iterates (4.1) so that, for all ℓ, $\partial_1 x^{(\ell)}(y, \theta)[\delta]$ (or, resp., $\partial_2 x^{(\ell)}(y, \theta)$) exists Lebesgue-a.e. Second, one may legitimately ask whether the sequence of weak derivatives converges, and what the properties of its cluster point are, if any, with respect to the weak derivatives at a minimizer $x^\star$.

Regarding weak differentiability of the iterates, this relies essentially on regularity conditions to apply the chain rule (e.g., [29, section 4.2.2]), i.e., regularity properties of the iteration mappings γ and ψ and of the initialization. For instance, for proximal splitting algorithms, it turns out that γ is the composition of one or several nonexpansive operators, hence 1-Lipschitz operators. In turn, γ is 1-Lipschitz. Furthermore, in all examples we consider, ψ is also 1-Lipschitz with respect to its second and third arguments. Therefore, if one starts at a Lipschitz continuous initialization, by induction, $y \mapsto x^{(\ell)}(y, \theta)$ and $\theta \mapsto x^{(\ell)}(y, \theta)$ are also Lipschitz. Using the chain rule for Lipschitz mappings (see [29, Theorem 4(ii) and the subsequent Remark, section 4.2.2]), weak differentiability of $x^{(\ell)}$ follows with respect to both arguments.

As far as convergence of the sequence of weak Jacobians is concerned, this remains an open question in the general case, and we believe this would necessitate intricate arguments from nonsmooth and variational analysis. This is left to future research.

From now on, we suppose that the Lipschitzian assumptions on γ, ψ, and the initial points hold. The next two sections detail the computation of $\partial_1 x^{(\ell)}(y, \theta)[\delta]$ and $\partial_2 x^{(\ell)}(y, \theta)$ in order to get the estimates $\mathrm{SURE}^{A}_{\mathrm{MC}}$ and $\mathrm{SUGAR}^{A}_{\mathrm{FDMC}}$.

4.2. Computation of $\mathrm{SURE}^{A}_{\mathrm{MC}}$ for risk optimization. We describe here the iterative computation of the directional derivative $\partial_1 x^{(\ell)}(y, \theta)[\delta]$ following the idea introduced in [70] (see section 2.4). Note that we focus on the directional derivative rather than the Jacobian

matrix itself. There are two reasons for this. The first is that we only need to have access to the trace of the Jacobian; the storage cost of the latter is, moreover, prohibitive. Second, it turns out that the trace of the Jacobian can be efficiently estimated by evaluating the weak directional derivatives at random directions δ (see section 2.3 for more details).

The next proposition summarizes a recursive scheme for computing the weak derivatives $\partial_1 x^{(\ell)}(y,\theta)[\delta]$.

Proposition 3. *For any vector $\delta \in \mathcal{X}$, the weak directional derivative $\mathcal{D}_x^{(\ell)} = \partial_1 x^{(\ell)}(y,\theta)[\delta]$ is given by*

$$\begin{aligned} \mathcal{D}_x^{(\ell)} &= \Gamma_a^{(\ell)}(\mathcal{D}_a^{(\ell)}) \\ \text{with} \quad \mathcal{D}_a^{(\ell+1)} &= \Psi_a^{(\ell)}(\mathcal{D}_a^{(\ell)}) + \Psi_y^{(\ell)}(\delta), \end{aligned}$$

where $\mathcal{D}_a^{(\ell)} = \partial_1 a^{(\ell)}(y,\theta)[\delta]$ and we have defined the linear mappings

$$\begin{aligned} \Gamma_a^{(\ell)}(\cdot) &= \partial_1 \gamma(a^{(\ell)})[\cdot], \\ \Psi_a^{(\ell)}(\cdot) &= \partial_1 \psi(a^{(\ell)}, y, \theta)[\cdot], \\ \Psi_y^{(\ell)}(\cdot) &= \partial_2 \psi(a^{(\ell)}, y, \theta)[\cdot]. \end{aligned}$$

Plugging $\partial_2 x^{(\ell)}(y,\theta)[\delta]$ into (2.4), and in turn into (2.2), gives iteratively an unbiased[4] estimate of the risk at the current iterate $x^{(\ell)}(y,\theta)$. The whole procedure is summarized in Figure 2. It is worth pointing out that although estimating the risk entails additional operations, the global complexity is the same as for the original iterative algorithm without risk estimation.

4.3. Computation of $\mathrm{SUGAR}^{A}_{\mathrm{FDMC}}$ for risk optimization. We now focus on the computation of the weak Jacobian $\partial_2 x^{(\ell)}(y,\theta)$. Unlike for risk estimation that required only weak directional derivatives, for risk optimization we need the full weak Jacobian matrix $\partial_2 x(y,\theta) \in \mathbb{R}^{\dim(\Theta)\times N}$. The proposed strategy, known as the forward accumulation, is one of the possible strategies for iteratively evaluating the derivatives by the use of the chain rule. The reverse accumulation is another strategy that does not require computing the full Jacobian matrix at the expense of a large memory load with respect to the number of iterations. Between these two extreme approaches, there are several hybrid strategies that can also be considered, knowing that finding the optimal Jacobian accumulation strategy is an NP-complete problem. Such strategies have been studied in the field of "automatic differentiation," and the reader is invited to see [35, 47] for a comprehensive account of these approaches.

In our case, we consider that, unlike for $\partial_1 x^{(\ell)}(y,\theta)$, the matrix $\partial_2 x(y,\theta)$ is in practice quite small since $\dim(\Theta) \ll P$, hence implying a memory load overhead of only a small fraction of P. Thus following the forward accumulation strategy, we propose a practical way to compute iteratively the full weak Jacobian matrix $\partial_2 x(y,\theta)$.

The next result describes an iterative scheme for computing $\partial_2 x^{(\ell)}(y,\theta)$.

[4]Expectation is to be taken here with respect to both the Gaussian measure of the noise W and the direction Δ.

Algorithm. Risk estimation of an iterative scheme.

Inputs: observation $y \in \mathcal{Y} = \mathbb{R}^P$, collection of parameters $\theta \in \Theta$
Parameters: noise variance $\sigma^2 > 0$, linear operator $\Phi \in \mathbb{R}^{P \times N}$, matrix $A \in \mathbb{R}^{M \times P}$, number $\mathcal{L}$ of iterations
Output: solution $x(y, \theta) \in \mathcal{X}$ and its risk estimate $\widehat{R}^A\{x\}(y, \theta)$

Sample a vector δ from $\mathcal{N}(0, \mathrm{Id}_P)$
Initialize $a^{(0)} \leftarrow 0$ *
Initialize $\mathcal{D}_a^{(0)} \leftarrow 0$
for ℓ from 0 to $\mathcal{L} - 1$ **do** *
  $a^{(\ell+1)} \leftarrow \psi(a^{(\ell)}, y, \theta)$ *
  $\mathcal{D}_a^{(\ell+1)} \leftarrow \Psi_a^{(\ell)}(\mathcal{D}_a^{(\ell)}) + \Psi_y^{(\ell)}(\delta)$
end for *
$x^{(\mathcal{L})} \leftarrow \gamma(a^{(\mathcal{L})})$ *
$\mathcal{D}_x^{(\mathcal{L})} \leftarrow \Gamma_a^{(\mathcal{L})}(\mathcal{D}_a^{(\mathcal{L})})$
$\widehat{df}{}^A_{\mathrm{MC}} \leftarrow \langle \Phi \mathcal{D}_x^{(\mathcal{L})} A^* A \delta \rangle$
$\mathrm{SURE}^A_{\mathrm{MC}} \leftarrow \left\| A(y - \Phi x^{(\mathcal{L})}) \right\|^2 - \sigma^2 \operatorname{tr}(A^* A) + 2\sigma^2 \widehat{df}{}^A_{\mathrm{MC}}$
return $x(y, \theta) \leftarrow x^{(\mathcal{L})}$ and $\widehat{R}^A\{x\}(y, \theta) \leftarrow \mathrm{SURE}^A_{\mathrm{MC}}$

Figure 2. *Pseudoalgorithm for risk estimation of an iterative scheme. The * symbols indicate the lines corresponding to the computation of x. The other lines are dedicated to the computation of the estimated risk $\widehat{R}^A$ using Monte-Carlo simulation. Even if computing the risk requires more operations, the global complexity of the algorithm is unchanged.*

Proposition 4. *The weak Jacobian $\mathcal{J}_x^{(\ell)} = \partial_2 x^{(\ell)}(y, \theta)$ is given by*

$$\mathcal{J}_x^{(\ell)} = \Gamma_a^{(\ell)}(\mathcal{J}_a^{(\ell)})$$
$$\text{with} \quad \mathcal{J}_a^{(\ell+1)} = \Psi_a^{(\ell)}(\mathcal{J}_a^{(\ell)}) + \Psi_\theta^{(\ell)},$$

where $\mathcal{J}_a^{(\ell)} = \partial_2 a^{(\ell)}(y, \theta)$ and we have defined

$$\Gamma_a^{(\ell)}(\cdot) = \partial_1 \gamma(a^{(\ell)})[\cdot],$$
$$\Psi_a^{(\ell)}(\cdot) = \partial_1 \psi(a^{(\ell)}, y, \theta)[\cdot],$$
$$\Psi_\theta^{(\ell)} = \partial_3 \psi(a^{(\ell)}, y, \theta).$$

Plugging $\partial_2 x^{(\ell)}(y, \theta)$ into the expression of $\mathrm{SUGAR}^A_{\mathrm{FDMC}}$ given by Proposition 1 provides iteratively an asymptotically (see Theorem 1) unbiased estimate of the gradient of the risk at the current iterate $x^{(\ell)}(y, \theta)$. The main steps of the procedure are summarized in Figure 3. The estimation of the gradient of the risk entails only a small computational overhead compared to the risk estimation approach of [51]. Their respective complexity remains the same, however.

Algorithm. Risk and gradient risk estimation of an iterative scheme.

Inputs: observation $y \in \mathcal{Y} = \mathbb{R}^P$, collection of parameters $\theta \in \Theta$
Parameters: noise variance $\sigma^2 > 0$, linear operator $\Phi \in \mathbb{R}^{P \times N}$, matrix $A \in \mathbb{R}^{M \times P}$, number $\mathcal{L}$ of iterations, decay parameters $C > 0$ and $0 < \alpha < 1$
Output: solution $x(y,\theta) \in \mathcal{X}$, its risk estimate $\widehat{R}^A\{x\}(y,\theta)$, and its gradient risk estimate $\hat{\nabla}_2 R^A\{x\}(y,\theta)$

Sample a vector δ from $\mathcal{N}(0, \mathrm{Id}_P)$ *
Choose $\varepsilon = C\sigma/P^\alpha$ *
for $y' = y$ and $y' = y + \varepsilon\delta$ **do** *
  Initialize $a^{(0)} \leftarrow 0$ *
  Initialize $\mathcal{J}_a^{(0)} \leftarrow 0$
  for ℓ from 0 to $\mathcal{L} - 1$ **do** *
    $a^{(\ell+1)} \leftarrow \psi(a^{(\ell)}, y', \theta)$ *
    $\mathcal{J}_a^{(\ell+1)} \leftarrow \Psi_a^{(\ell)}(\mathcal{J}_a^{(\ell)}) + \Psi_\theta^{(\ell)}$
  end for *
  $x^{(\ell)}(y') \leftarrow \gamma(a^{(\ell)})$ *
  $\mathcal{J}_x^{(\ell)}(y') \leftarrow \Gamma_a^{(\ell)}(\mathcal{J}_a^{(\ell)})$
end for *
$\widehat{df}_{\mathrm{FDMC}} \leftarrow \frac{1}{\varepsilon}\left\langle \Phi(x^{(\mathcal{L})}(y+\varepsilon\delta) - x^{(\mathcal{L})}(y)),\ A^*A\delta \right\rangle$ *
$\mathrm{SURE}^A_{\mathrm{FDMC}} \leftarrow \left\|A(y - \Phi x^{(\mathcal{L})})\right\|^2 - \sigma^2 \operatorname{tr}(A^*A) + 2\sigma^2 \widehat{df}_{\mathrm{FDMC}}$ *
$\mathrm{SUGAR}^A_{\mathrm{FDMC}} \leftarrow 2\mathcal{J}_x^{(\mathcal{L})}(y)^*\Phi^*A^*A(\Phi x^{(\mathcal{L})} - y) + \frac{2\sigma^2}{\varepsilon}(\mathcal{J}_x^{(\mathcal{L})}(y+\varepsilon\delta) - \mathcal{J}_x^{(\mathcal{L})}(y))^*\Phi^*A^*A\delta$
return $x(y,\theta) \leftarrow x^{(\mathcal{L})}(y)$, $\widehat{R}^A\{x\}(y,\theta) \leftarrow \mathrm{SURE}^A_{\mathrm{FDMC}}$ and $\hat{\nabla}_2 R^A\{x\}(y,\theta) \leftarrow \mathrm{SUGAR}^A_{\mathrm{FDMC}}$

Figure 3. *Pseudoalgorithm for risk and gradient risk estimation of an iterative scheme. The * symbols indicate the lines corresponding to the computation of x and its estimated risk R^A using approximated Monte-Carlo simulation, i.e., as described in [51]. The other lines are dedicated to the computation of the estimated gradient of the risk $\hat{\nabla} R^A$. Even if computing the gradient of the risk requires more operations, the global complexity of the algorithm is unchanged.*

Finally, note that in both schemes, an initialization other than $a^{(0)} = 0$ can be chosen, for instance, one depending on y and θ, in which case the respective derivatives must be initialized accordingly.

The following sections are devoted to instantiating this approach to more specific iterative algorithms that are able to handle nonsmooth convex objective functions E.

4.4. Application to generalized forward-backward splitting. The generalized forward-fackward (GFB) splitting [50] allows one to find one element belonging to the set $x(y,\theta)$ solution of the structured convex optimization problem

$$x(y,\theta) = \operatorname*{Argmin}_{x \in \mathcal{X}} \left\{ E(x,y,\theta) = F(x,y,\theta) + \sum_{k=1}^{Q} G_k(x,y,\theta) \right\} \tag{4.2}$$

under the assumptions that all functions are proper, closed, and convex, F is $C^1(\mathcal{X})$ with L-Lipschitz continuous gradient, and the G_k functions are simple, in the sense that their proximal operator can be computed in closed form (e.g., the ℓ_1-norm is simple since its proximal operator is explicitly the soft-thresholding). Recall that the proximal mapping of a proper closed convex function G is defined as

$$\mathrm{Prox}_G : x \in \mathcal{X} \mapsto \underset{z\in\mathcal{X}}{\mathrm{Argmin}}\ \frac{1}{2}\|z-x\|^2 + G(z).$$

This mapping is uniquely valued and nonexpansive (i.e., $\|\mathrm{Prox}_G(x_1) - \mathrm{Prox}_G(x_2)\| \leqslant \|x_1 - x_2\|$ for any $x_1, x_2 \in \mathcal{X}$), in fact even firmly so.

The GFB splitting implements iteration (4.1) with $a^{(\ell)} = (\xi^{(\ell)}, z_1^{(\ell)}, \ldots, z_Q^{(\ell)}) \in \mathcal{A} = \mathcal{X}^{1+Q}$, $x^{(\ell)} = \gamma(a^{(\ell)}) = \xi^{(\ell)}$, and $a^{(\ell+1)} = \psi(a^{(\ell)}, y, \theta)$ chosen such that for all $k = 1, \ldots, Q$,

$$\begin{aligned} x^{(\ell+1)} &= \tfrac{1}{Q}\sum_{k=1}^{Q} z_k^{(\ell+1)}, \\ z_k^{(\ell+1)} &= z_k^{(\ell)} - x^{(\ell)} + \mathrm{Prox}_{\nu Q G_k}(\mathcal{Z}_k^{(\ell)}, y, \theta) \\ \text{with}\quad \mathcal{Z}_k^{(\ell)} &= 2x^{(\ell)} - z_k^{(\ell)} - \nu\nabla_1 F(x^{(\ell)}, y, \theta). \end{aligned}$$

With the parameter $\nu \in]0, 2/L[$, the sequence of iterates $x^{(\ell)}$ is provably guaranteed to converge to a minimizer $x(y,\theta)$ of (4.2). One recovers as special cases the FB splitting [14] when $Q = 1$ and the Douglas–Rachford splitting [12] when $F = 0$.

Corollary 1. *For any vector $\delta \in \mathcal{X}$, the GFB weak directional derivatives $\mathcal{D}_x^{(\ell)} = \Gamma_a^{(\ell)}(\mathcal{D}_a^{(\ell)})$ and $\mathcal{D}_a^{(\ell+1)} = \Psi_a^{(\ell)}(\mathcal{D}_a^{(\ell)}) + \Psi_y^{(\ell)}(\delta)$ are computed by evaluating iteratively*

$$\begin{aligned} \mathcal{D}_x^{(\ell+1)} &= \tfrac{1}{Q}\sum_{k=1}^{Q} \mathcal{D}_{z_k}^{(\ell+1)}, \\ \mathcal{D}_{z_k}^{(\ell+1)} &= \mathcal{D}_{z_k}^{(\ell)} - \mathcal{D}_x^{(\ell)} + \mathcal{G}_{k,x}^{(\ell)}(\mathcal{D}_{\mathcal{Z}_k}^{(\ell)}) + \mathcal{G}_{k,y}^{(\ell)}(\delta) \\ \textit{with}\quad \mathcal{D}_{\mathcal{Z}_k}^{(\ell)} &= 2\mathcal{D}_x^{(\ell)} - \mathcal{D}_{z_k}^{(\ell)} - \nu(\mathcal{F}_x^{(\ell)}(\mathcal{D}_x^{(\ell)}) + \mathcal{F}_y^{(\ell)}(\delta)), \end{aligned}$$

where we have defined the following linear mappings:

$$\begin{aligned} \mathcal{G}_{k,x}^{(\ell)}(\cdot) &= \partial_1\{\mathrm{Prox}_{\nu Q G_k}\}(\mathcal{Z}_k^{(\ell)}, y, \theta)[\cdot], \\ \mathcal{G}_{k,y}^{(\ell)}(\cdot) &= \partial_2\{\mathrm{Prox}_{\nu Q G_k}\}(\mathcal{Z}_k^{(\ell)}, y, \theta)[\cdot], \\ \mathcal{F}_x^{(\ell)}(\cdot) &= \partial_1\{\nabla_1 F\}(x^{(\ell)}, y, \theta)[\cdot], \\ \mathcal{F}_y^{(\ell)}(\cdot) &= \partial_2\{\nabla_1 F\}(x^{(\ell)}, y, \theta)[\cdot]. \end{aligned}$$

Corollary 2. *The GFB weak Jacobian $\mathcal{J}_x^{(\ell)} = \Gamma_a^{(\ell)}(\mathcal{J}_a^{(\ell)})$, where $\mathcal{J}_a^{(\ell+1)} = \Psi_a^{(\ell)}(\mathcal{J}_a^{(\ell)}) + \Psi_\theta^{(\ell)}$,*

is computed by evaluating iteratively

$$\begin{aligned} \mathcal{J}_x^{(\ell+1)} &= \tfrac{1}{Q}\sum_{k=1}^{Q} \mathcal{J}_{z_k}^{(\ell+1)}, \\ \mathcal{J}_{z_k}^{(\ell+1)} &= \mathcal{J}_{z_k}^{(\ell)} - \mathcal{J}_x^{(\ell)} + \mathcal{G}_{k,x}^{(\ell)}(\mathcal{J}_{\mathcal{Z}_k}^{(\ell)}) + \mathcal{G}_{k,\theta}^{(\ell)} \\ \text{with}\quad \mathcal{J}_{\mathcal{Z}_k}^{(\ell)} &= 2\mathcal{J}_x^{(\ell)} - \mathcal{J}_{z_k}^{(\ell)} - \nu(\mathcal{F}_x^{(\ell)}(\mathcal{J}_x^{(\ell)}) + \mathcal{F}_\theta^{(\ell)}), \end{aligned}$$

where we have defined

$$\begin{aligned} \mathcal{G}_{k,x}^{(\ell)}(\cdot) &= \partial_1\{\mathrm{Prox}_{\nu Q G_k}\}(\mathcal{Z}_k^{(\ell)}, y, \theta)[\cdot], \\ \mathcal{G}_{k,\theta}^{(\ell)} &= \partial_3\{\mathrm{Prox}_{\nu Q G_k}\}(\mathcal{Z}_k^{(\ell)}, y, \theta), \\ \mathcal{F}_x^{(\ell)}(\cdot) &= \partial_1\{\nabla_1 F\}(x^{(\ell)}, y, \theta)[\cdot], \\ \mathcal{F}_\theta^{(\ell)} &= \partial_3\{\nabla_1 F\}(x^{(\ell)}, y, \theta). \end{aligned}$$

4.5. Application to primal-dual splitting. Proximal splitting schemes can be used to find an element of the set $x(y,\theta)$ defined as the solution of the large class of variational problems

$$x(y,\theta) = \operatorname*{Argmin}_{x\in\mathcal{X}} \{E(x,y,\theta) = H(x,y,\theta) + G(K(x),y,\theta)\}, \tag{4.3}$$

where both $x \mapsto H(x,y,\theta)$ and $u \mapsto G(u,y,\theta)$ are proper closed convex and simple functions and $K : \mathcal{X} \to \mathcal{U}$ is a bounded linear operator.

The primal-dual[5] relaxed Arrow–Hurwicz algorithm, revitalized recently in [10] (which we coin "CP") to solve (4.3), implements (4.1) with $a^{(\ell)} = (\xi^{(\ell)}, \tilde{x}^{(\ell)}, u^{(\ell)}) \in \mathcal{A} = \mathcal{X}^2 \times \mathcal{U}$, $x^{(\ell)} = \gamma(a^{(\ell)}) = \xi^{(\ell)}$, and $a^{(\ell+1)} = \psi(a^{(\ell)}, y, \theta)$ such that

$$\begin{aligned} u^{(\ell+1)} &= \mathrm{Prox}_{\tau G^*}(U^{(\ell)}, y, \theta), \quad \text{where} \quad U^{(\ell)} = u^{(\ell)} + \tau K(\tilde{x}^{(\ell)}), \\ x^{(\ell+1)} &= \mathrm{Prox}_{\xi H}(X^{(\ell)}, y, \theta), \quad \text{where} \quad X^{(\ell)} = x^{(\ell)} - \xi K^*(u^{(\ell+1)}), \\ \tilde{x}^{(\ell+1)} &= x^{(\ell+1)} + \zeta(x^{(\ell+1)} - x^{(\ell)}), \end{aligned} \tag{4.4}$$

where the Legendre–Fenchel conjugate of G is defined as $G^*(u,y,\tau) = \max_z \langle z, u\rangle - G(z,y,\tau)$ and its proximal operator is given by Moreau's identity as

$$\mathrm{Prox}_{\tau G^*}(u,y) = u - \tau\,\mathrm{Prox}_{G/\tau}(u/\tau, y).$$

The parameters $\tau > 0$, $\xi > 0$ are chosen such that $\tau\xi\,\|K\|^2 < 1$, and $\zeta \in [0,1]$ to ensure provable convergence of $x^{(\ell)}$ toward an element in the set $x(y,\theta)$ of (4.3). $\zeta = 0$ corresponds to the Arrow–Hurwitz algorithm, and for $\zeta = 1$, a sublinear $O(1/\ell)$ convergence rate on the partial duality gap was established in [10].

[5] We invite the interested reader to consult [41] for a detailed review on primal-dual algorithms.

Corollary 3. *For any vector $\delta \in \mathcal{X}$, the CP weak directional derivatives $\mathcal{D}_x^{(\ell)} = \Gamma_a^{(\ell)}(\mathcal{D}_a^{(\ell)})$ and $\mathcal{D}_a^{(\ell+1)} = \Psi_a^{(\ell)}(\mathcal{D}_a^{(\ell)}) + \Psi_y^{(\ell)}(\delta)$ are computed by evaluating iteratively*

$$\begin{aligned}
\mathcal{D}_u^{(\ell+1)} &= \mathcal{G}_u^{(\ell)}(\mathcal{D}_U^{(\ell)}) + \mathcal{G}_y^{(\ell)}(\delta), \quad \text{where} \quad \mathcal{D}_U^{(\ell)} = \mathcal{D}_u^{(\ell)} + \tau K(\mathcal{D}_{\tilde{x}}^{(\ell)}),\\
\mathcal{D}_x^{(\ell+1)} &= \mathcal{H}_x^{(\ell)}(\mathcal{D}_X^{(\ell)}) + \mathcal{H}_y^{(\ell)}(\delta), \quad \text{where} \quad \mathcal{D}_X^{(\ell)} = \mathcal{D}_x^{(\ell)} - \xi K^*(\mathcal{D}_u^{(\ell+1)}),\\
\mathcal{D}_{\tilde{x}}^{(\ell+1)} &= \mathcal{D}_x^{(\ell+1)} + \zeta(\mathcal{D}_x^{(\ell+1)} - \mathcal{D}_x^{(\ell)}),
\end{aligned}$$

where we have defined the following linear mappings:

$$\begin{aligned}
\mathcal{H}_x^{(\ell)}(\cdot) &= \partial_1\{\mathrm{Prox}_{\xi H}\}(X^{(\ell)}, y, \theta)[\cdot],\\
\mathcal{H}_y^{(\ell)}(\cdot) &= \partial_2\{\mathrm{Prox}_{\xi H}\}(X^{(\ell)}, y, \theta)[\cdot],\\
\mathcal{G}_u^{(\ell)}(\cdot) &= \partial_1\{\mathrm{Prox}_{\tau G^*}\}(U^{(\ell)}, y, \theta)[\cdot],\\
\mathcal{G}_y^{(\ell)}(\cdot) &= \partial_2\{\mathrm{Prox}_{\tau G^*}\}(U^{(\ell)}, y, \theta)[\cdot].
\end{aligned}$$

Corollary 4. *Similarly to Corollary 3, the CP weak Jacobians $\mathcal{J}_x^{(\ell)} = \Gamma_a^{(\ell)}(\mathcal{J}_a^{(\ell)})$ and $\mathcal{J}_a^{(\ell+1)} = \Psi_a^{(\ell)}(\mathcal{J}_a^{(\ell)}) + \Psi_\theta^{(\ell)}$ are computed by evaluating iteratively*

$$\begin{aligned}
\mathcal{J}_u^{(\ell+1)} &= \mathcal{G}_u^{(\ell)}(\mathcal{J}_U^{(\ell)}) + \mathcal{G}_\theta^{(\ell)}, \quad \text{where} \quad \mathcal{J}_U^{(\ell)} = \mathcal{J}_u^{(\ell)} + \tau K(\mathcal{J}_{\tilde{x}}^{(\ell)}),\\
\mathcal{J}_x^{(\ell+1)} &= \mathcal{H}_x^{(\ell)}(\mathcal{J}_X^{(\ell)}) + \mathcal{H}_\theta^{(\ell)}, \quad \text{where} \quad \mathcal{J}_X^{(\ell)} = \mathcal{J}_x^{(\ell)} - \xi K^*(\mathcal{J}_u^{(\ell+1)}),\\
\mathcal{J}_{\tilde{x}}^{(\ell+1)} &= \mathcal{J}_x^{(\ell+1)} + \zeta(\mathcal{J}_x^{(\ell+1)} - \mathcal{J}_x^{(\ell)}),
\end{aligned}$$

where we have defined

$$\begin{aligned}
\mathcal{H}_x^{(\ell)}(\cdot) &= \partial_1\{\mathrm{Prox}_{\xi H}\}(X^{(\ell)}, y, \theta)[\cdot],\\
\mathcal{H}_\theta^{(\ell)} &= \partial_3\{\mathrm{Prox}_{\xi H}\}(X^{(\ell)}, y, \theta),\\
\mathcal{G}_u^{(\ell)}(\cdot) &= \partial_1\{\mathrm{Prox}_{\tau G^*}\}(U^{(\ell)}, y, \theta)[\cdot],\\
\mathcal{G}_\theta^{(\ell)} &= \partial_3\{\mathrm{Prox}_{\tau G^*}\}(U^{(\ell)}, y, \theta).
\end{aligned}$$

Note that the two proximal splitting schemes described here were chosen for their flexibility and the richness of the class of problems they can handle. Obviously, the methodology and discussion extend easily to the reader's favorite proximal splitting algorithm.

5. Examples and numerical results.

In this section, we exemplify the use of the formal differentiation of iterative proximal splitting algorithms for three popular variational problems: nuclear norm regularization, total variation regularization, and the multiscale wavelet ℓ_1-analysis sparsity prior. For each of these, the expressions of all quantities including the proximal operators and their derivatives are given in closed form. For each problem, we illustrate the usefulness of our gradient risk estimators for (multi-) continuous parameter optimization.

5.1. Implementation details.

All experiments reported below are based on the algorithms detailed in Figures 2 and 3 in conjunction with proximal splitting algorithms presented in the previous section. The step of the finite difference is chosen as $\varepsilon = 2\sigma/P^{0.3}$. Iterative proximal

splitting algorithms will be used with $\mathcal{L} = 100$ iterations. For quasi-Newton optimization, we used the Broyden–Fletcher–Goldfarb–Shanno (BFGS) method with the implementation of [42]. The use of BFGS is just given as an example to make the most of the proposed gradient estimator of the risk and seems to be good enough for the cases considered in all of the following experiment examples. Of course, other first-order optimization methods can be considered just as well, essentially if the risk presents several local minima.

An important issue in using quasi-Newton optimization is the choice of the initialization, the initial step, and the stopping criteria. For a variation regularization problem expressed as

$$\operatorname*{Argmin}_x \frac{1}{2}\|\Phi x - y\|^2 + \sum_{k=1}^{K} \lambda^k \mathcal{R}^k(x), \tag{5.1}$$

where $\lambda^k > 0$ for all $k \in \mathbb{N}$, the initialization λ_0^k is chosen empirically as

$$\lambda_0^k = \frac{P\sigma^2}{4\sum_{k=1}^{K} \mathcal{R}^k(x_{\mathrm{LS}}(y))}, \tag{5.2}$$

where $x_{\mathrm{LS}}(y)$ is the least-squares estimator. At the first iteration, the approximate inverse Hessian B_1 should be chosen such that, for all $k > 0$, λ_1^k is of the same order as λ_0^k. To this end, we suggest initializing B_1 as a diagonal matrix with diagonal entries

$$B_1^k = \left| \frac{\alpha \lambda_0^k}{\mathrm{SUGAR}^A_{\mathrm{FDMC}}\{x\}(y, \lambda_0, \delta, \varepsilon)_k} \right| \tag{5.3}$$

such that, for all k, $\lambda_1^k = (1 \pm \alpha)\lambda_0^k$, where, in practice, we have chosen $\alpha = 0.9$. Finally, the BFGS method stops after the following criterion is reached:

$$\frac{\left\|\mathrm{SUGAR}^A_{\mathrm{FDMC}}\{x\}(y, \lambda_n, \delta, \varepsilon)\right\|_\infty}{\left\|\mathrm{SUGAR}^A_{\mathrm{FDMC}}\{x\}(y, \lambda_0, \delta, \varepsilon)\right\|_\infty} \leqslant \tau, \tag{5.4}$$

where we have chosen $\tau = 0.02$, meaning that the algorithm stops if all (weak) partial derivatives are at least 50 times lower than the maximal one at initialization.

For the sake of reproducibility, the MATLAB scripts implementing the SURE and the SUGAR for the different problems described hereafter are available online at http://www.math.u-bordeaux1.fr/~cdeledal/sugar.php.

5.2. Nuclear norm regularization. We consider the recovery of a low-rank matrix $x_0 \in \mathbb{R}^{n_1 \times n_2}$ from an observation $y \in \mathbb{R}^P$ of $Y = \Phi x_0 + W$, $W \sim \mathcal{N}(0, \sigma^2 \mathrm{Id}_P)$, where we have identified the matrix space $\mathbb{R}^{n_1 \times n_2}$ to the vector space $\mathbb{R}^N$ with $N = n_1 n_2$. To this end, we consider the following spectral regularization problem:

$$x^\star(y, \lambda) \in \operatorname*{Argmin}_x \frac{1}{2}\|\Phi x - y\|^2 + \lambda \|x\|_*, \tag{5.5}$$

where $\lambda > 0$ and $\|\cdot\|_*$ is the nuclear norm (also known as trace for the symmetric semidefinite positive case or Schatten 1-norm). This is a spectral function defined as the ℓ_1-norm of the singular values $\Lambda_x \in \mathbb{R}^{n=\min(n_1,n_2)}$, i.e.,

$$\|x\|_* = \|\Lambda_x\|_1 .$$

The nuclear norm is a particular case of spectral regularization that accounts for prior knowledge of the spectrum of x, typically low-rank (see, e.g., [30]). It is the convex hull of the rank function restricted to the unit spectral ball [8]. The parameter λ balances the sparsity of the spectrum of the recovered matrix and the tolerated amount of noise. However, except in the random measurements setting, there is no direct relation between λ and the rank of $x(y,\lambda)$. The optimal value of λ indeed depends on x_0, Φ, and σ, confirming the importance of automatic selection procedures.

Problem (5.5) is a special instance of (4.2) with the parameter $\lambda = \theta \in \Theta = \mathbb{R}^+$, $Q = 1$, and

$$\begin{aligned} F(x,y,\lambda) &= \frac{1}{2}\left\|\Phi x - y\right\|^2, \\ G_1(x,y,\lambda) &= \lambda \left\|x\right\|_*. \end{aligned}$$

Hence the GFB algorithm[6] can be used to solve (5.5) by setting

$$\begin{aligned} \nabla_1 F(x,y,\lambda) &= \Phi^*(\Phi x - y), \\ \mathrm{Prox}_{\tau G_1}(x,y,\lambda) &= V_x \,\mathrm{diag}(\mathrm{ST}(\Lambda_x, \tau\lambda)) U_x^*, \end{aligned}$$

where $\mathrm{diag} : \mathbb{R}^n \to \mathbb{R}^{n_1 \times n_2}$ maps the entries of a vector in $\mathbb{R}^n$ to the main diagonal of a rectangular matrix in $\mathbb{R}^{n_1 \times n_2}$ filled with 0 elsewhere, $(V_x, U_x, \Lambda_x) \in \mathbb{R}^{n_1 \times n_1} \times \mathbb{R}^{n_2 \times n_2} \times \mathbb{R}^n$ is the singular value decomposition of x such that $x = V_x \,\mathrm{diag}(\Lambda_x) U_x^*$, and ST is the soft-thresholding operator (3.1). Corollaries 1 and 2 can then be applied using, for any $\delta_x \in \mathcal{X}$ and $\delta_y \in \mathcal{Y}$, the relations

$$\begin{aligned} \partial_1\{\nabla_1 F\}(x,y,\lambda)[\delta_x] &= \Phi^*\Phi\delta_x, \\ \partial_2\{\nabla_1 F\}(x,y,\lambda)[\delta_y] &= -\Phi^*\delta_y, \\ \partial_3\{\nabla_1 F\}(x,y,\lambda) &= 0, \\ \partial_1\{\mathrm{Prox}_{\tau G_1}\}(x,y,\lambda)[\delta_x] &= V_x(\mathcal{H}(\Lambda_x)[\bar{\delta}_x] + \Gamma_S(\Lambda_x)[\bar{\delta}_x] + \Gamma_A(\Lambda_x)[\bar{\delta}_x]) U_x^*, \\ \partial_2\{\mathrm{Prox}_{\tau G_1}\}(x,y,\lambda)[\delta_y] &= 0, \\ \partial_3\{\mathrm{Prox}_{\tau G_1}\}(x,y,\lambda) &= V_x \,\mathrm{diag}(\partial_2 \mathrm{ST}(\Lambda_x, \tau\lambda)) U_x^*, \end{aligned}$$

where $\bar{\delta}_x = V_X^* \delta_x U_X \in \mathbb{R}^{n_1 \times n_2}$, $\mathcal{H}(\Lambda_x)$ is defined as

$$\mathcal{H}(\Lambda_x)[\bar{\delta}_x] = \mathrm{diag}(\partial_1 \mathrm{ST}(\Lambda_x, \rho\lambda)[\mathrm{diag}(\bar{\delta}_x)]),$$

and $\Gamma_S(\Lambda_x)$ and $\Gamma_A(\Lambda_x)$ are defined, for all $1 \leqslant i \leqslant n_1$ and $1 \leqslant j \leqslant n_2$, as

$$\Gamma_S(\Lambda_x)[\bar{\delta}_x]_{i,j} = \frac{(\bar{\delta}_x)_{i,j} + (\bar{\delta}_x)_{j,i}}{2} \times \begin{cases} 0 & \text{if} \quad i = j, \\ \frac{\mathrm{ST}(\Lambda_x,\rho\lambda)_i - \mathrm{ST}(\Lambda_x,\rho\lambda)_j}{(\Lambda_x)_i - (\Lambda_x)_j} & \text{if} \quad (\Lambda_x)_i \neq (\Lambda_x)_j, \\ \partial_1 \mathrm{ST}(\Lambda_x, \rho\lambda)_{i,i} & \text{otherwise,} \end{cases}$$

$$\Gamma_A(\Lambda_x)[\bar{\delta}_x]_{i,j} = \frac{(\bar{\delta}_x)_{i,j} - (\bar{\delta}_x)_{j,i}}{2} \times \begin{cases} 0 & \text{if} \quad i = j, \\ \frac{\mathrm{ST}(\Lambda_x,\rho\lambda)_i + \mathrm{ST}(\Lambda_x,\rho\lambda)_j}{(\Lambda_x)_i + (\Lambda_x)_j} & \text{if} \quad (\Lambda_x)_i > 0 \quad \text{or} \quad (\Lambda_x)_j > 0, \\ \partial_1 \mathrm{ST}(\Lambda_x, \rho\lambda)_{i,i} & \text{otherwise,} \end{cases}$$

[6] In this case where $Q = 1$, this corresponds to the FB algorithm.

where for $i > n$ we have extended Λ_x and $\mathrm{ST}(\Lambda_x, \rho\lambda)$ as $(\Lambda_x)_i = 0$ and $\mathrm{ST}(\Lambda_x, \rho\lambda)_i = 0$, and for $j > n_1$ or $i > n_2$, $\bar{\delta}_x$ as $(\bar{\delta}_x)_{j,i} = 0$. Recall from (A.2) that the weak derivatives of the soft-thresholding are defined, for $t \in \mathbb{R}^N$, $\rho > 0$, $\delta_t \in \mathbb{R}^N$, $1 \leqslant i \leqslant N$, by

$$\partial_1 \mathrm{ST}(t,\rho)_{i,i} = \begin{cases} 0 & \text{if} \quad |t_i| \leqslant \rho, \\ 1 & \text{otherwise,} \end{cases} \tag{5.6}$$

$$\partial_1 \mathrm{ST}(t,\rho)[\delta_t]_i = \partial_1 \mathrm{ST}(t,\rho)_{i,i} \times (\delta_t)_i,$$

$$\partial_2 \mathrm{ST}(t,\rho)_i = \begin{cases} 0 & \text{if} \quad |t_i| \leqslant \rho, \\ -\operatorname{sign}(t_i) & \text{otherwise.} \end{cases}$$

The closed-form expression we derived for $\partial_1\{\mathrm{Prox}_{\tau G_1}\}(x, y, \lambda)[\delta_x]$ is far from trivial. It is essentially due to [26, 43, 63]; see [9] for an expression similar to ours. The generalization of this result to other matrix-valued spectral functions has been studied in [20].

Application to matrix completion. We illustrate the nuclear norm regularization on a matrix completion problem encountered in recommendation systems such as the popular Netflix problem [5]. We therefore consider $y \in \mathbb{R}^P$ with the forward model $Y = \Phi x_0 + W$, $W \sim \mathcal{N}(0, \sigma^2 \mathrm{Id}_P)$, where x_0 is a dense but low-rank (or approximately so) matrix and Φ is a binary masking operator.

We have taken $(n_1, n_2) = (1000, 100)$ and $P = 25000$ observed entries (i.e., 25%). The underlying matrix $x_0 = V_{x_0} \operatorname{diag} \Lambda_{x_0} U_{x_0}^*$ has been chosen with V_{x_0} and U_{x_0}, two realizations of the uniform distribution of orthogonal matrices, and $\Lambda_{x_0} = (k^{-1})_{1 \leqslant k \leqslant n}$ such that x_0 is approximately low-rank with a rapidly decaying spectrum. The binary masking operator is such that for $i = 1, \ldots, P$, $(\Phi x)_i = x_{\Sigma(i)_1, \Sigma(i)_2}$, where $\Sigma : [1, \ldots, n_1 \times n_2] \to [1, \ldots, n_1] \times [1, \ldots, n_2]$ is the realization of a random permutation of the $n_1 \times n_2$ entries of x. The standard deviation σ has been set such that the resulting minimum least-squares estimate $x_{\mathrm{LS}}(y) = \Phi^* y$ has a relative error $\|x_{\mathrm{LS}}(y) - x_0\|_F / \|x_0\|_F = 0.9$.

Figures 4(a) and 4(b) depict the risk, the prediction risk, and the SURE $= \mathrm{SURE}^A$ (with $A = \mathrm{Id}$) estimates[7] as functions of λ obtained from a single realization of y and δ. In Figure 4(a), $\mathrm{SURE}_{\mathrm{MC}}\{x\}(y, \lambda, \delta)$ has been evaluated for 12 values of λ chosen in a suitable tested range using the algorithm given in Figure 2. Figure 4(b) shows the benefit of computing $\mathrm{SURE}_{\mathrm{FDMC}}\{x\}(y, \lambda, \delta, \varepsilon)$ and $\mathrm{SUGAR}_{\mathrm{FDMC}}\{x\}(y, \lambda, \delta, \varepsilon)$, as described in Figure 3, to realize a quasi-Newton optimization. The sequence of iterates λ_n is represented, as well as the sequence of the slopes of $\mathrm{SURE}_{\mathrm{FDMC}}\{x\}(y, \lambda_n, \delta, \varepsilon)$ given by $\mathrm{SUGAR}_{\mathrm{FDMC}}\{x\}(y, \lambda_n, \delta, \varepsilon)$. The BFGS algorithm reaches the optimal value in only five iterations. One can also notice that $\mathrm{SURE}_{\mathrm{FDMC}}\{x\}(y, \lambda, \delta, \varepsilon)$ and $\mathrm{SURE}_{\mathrm{MC}}\{x\}(y, \lambda, \delta)$ are both good—and visually equivalent—estimators of the prediction risk. At the optimum value $\lambda^\star$ minimizing the SURE, the true risk is not too far from its minimum, showing that, in this case, the prediction risk is indeed a good objective in order to minimize the risk. In Figure 4(c) a zoom-in on the solution $x(y, \lambda^\star)$ is compared to x_0 and $x_{\mathrm{LS}}(y)$, and their respective spectra are shown in Figure 4(d). The solution $x(y, \lambda^\star)$ has a rank of 57 with a relative error of 0.45 (i.e., a gain of about a factor 2 with respect to the least-squares estimator).

[7] Without impacting the optimal choice of λ, the curves have been rescaled for visualization purposes.

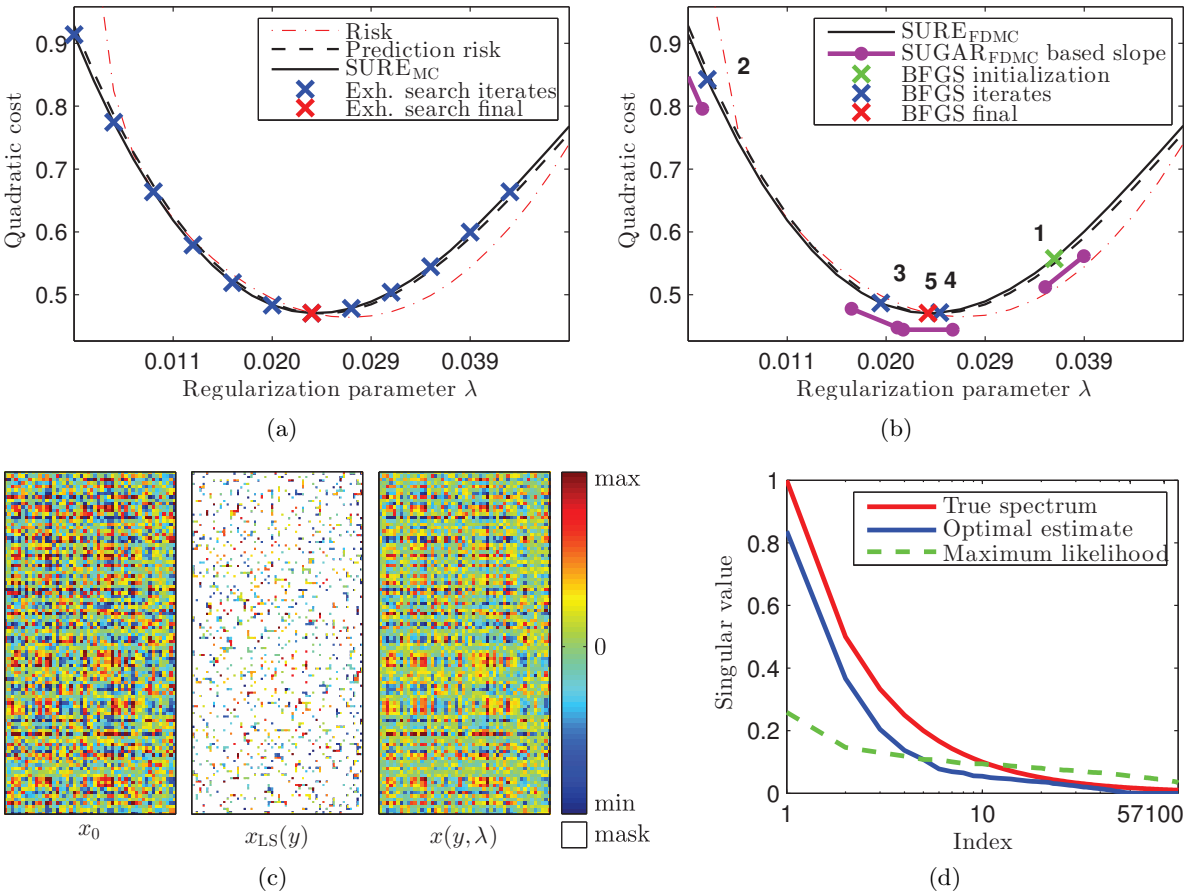

Figure 4. (a)–(b) *Risk, prediction risk, and the* SURE *estimates*[7] *as functions of the regularization parameter* λ. (a) *The* 12 *points where* $\mathrm{SURE}_{\mathrm{MC}}\{x\}(y,\lambda,\delta)$ *has been evaluated by exhaustive search.* (b) *The five evaluation points of* $\mathrm{SURE}_{\mathrm{FDMC}}\{x\}(y,\lambda,\delta,\varepsilon)$ *and* $\mathrm{SUGAR}_{\mathrm{FDMC}}\{x\}(y,\lambda,\delta,\varepsilon)$ *required by BFGS to reach the optimal* λ. (c)–(d) *Respectively, a zoom-in and the spectra of the underlying matrix* x_0, *the least-squares estimate* $x_{\mathrm{LS}}(y)$, *and the solution* $x(y,\lambda)$ *at the optimal* λ.

5.3. Total variation regularization. We consider the recovery of a piecewise constant two-dimensional image $x_0 \in \mathbb{R}^{n_1 \times n_2}$ from an observation y of $Y = \Phi x_0 + W \in \mathbb{R}^P$, $W \sim \mathcal{N}(0, \sigma^2 \mathrm{Id}_P)$, where we have identified the image space $\mathbb{R}^{n_1 \times n_2}$ to the vector space $\mathbb{R}^N$ with $N = n_1 n_2$. To this end, we suggest using (isotropic) total variation regularization of the form

$$x^\star(y,\lambda) \in \operatorname*{Argmin}_x \frac{1}{2}\|\Phi x - y\|^2 + \lambda \|\tilde{\nabla} x\|_{1,2}, \tag{5.7}$$

where $\lambda > 0$ and $\tilde{\nabla} : \mathbb{R}^N \to \mathbb{R}^{N \times 2}$ is the two-dimensional discrete gradient operator. The ℓ^1-ℓ^2–norm of a vector field $t = (t_i)_{i=1}^N \in \mathbb{R}^{N \times 2}$, with $t_i \in \mathbb{R}^2$, is defined as $\|t\|_{1,2} = \sum_i \|t_i\|$. Total variation promotes the sparsity of the gradient field, which turns out to be a prior that enforces smoothing while preserving edges. The parameter λ controls the regularity of the image. A large value of λ results in an image with large homogeneous areas, while a small value

results in an image with several small disconnected regions. The optimal value of λ is image- and degradation-dependent, revealing the importance of automatic selection procedures.

Problem (5.7) is a special instance of (4.2) using $x = (f, u) \in \mathcal{X} = \mathbb{R}^N \times \mathbb{R}^{N\times 2}$, the parameter $\lambda = \theta \in \Theta = \mathbb{R}^+$, $Q = 2$ simple functionals, and for $x = (f, u)$

$$\begin{aligned} F(x, y, \lambda) &= \frac{1}{2} \|\Phi f - y\|^2 , \\ G_1(x, y, \lambda) &= \lambda \|u\|_{1,2} , \\ G_2(x, y, \lambda) &= \iota_{\mathcal{C}}(x), \quad \text{where} \quad \mathcal{C} = \left\{ x = (f, u) \setminus u = \tilde{\nabla} f \right\}. \end{aligned}$$

Hence the GFB algorithm can be used to solve (5.7) using

$$\begin{aligned} \nabla_1 F(x, y, \lambda) &= (\Phi^*(\Phi f - y), 0), \\ \mathrm{Prox}_{\tau G_1}(x, y, \lambda) &= (f, \mathrm{ST}_{1,2}(u, \tau\lambda)), \\ \mathrm{Prox}_{\tau G_2}(x, y, \lambda) &= ((\mathrm{Id} + \Delta)^{-1}(f + \operatorname{div} u), \tilde{\nabla}(\mathrm{Id} + \Delta)^{-1}(f + \operatorname{div} u)), \end{aligned}$$

where Δ is the Laplacian operator and div is the discrete divergence operator such that $\operatorname{div} = -\tilde{\nabla}^*$. The operator $\mathrm{ST}_{1,2}$ is the componentwise ℓ^1-ℓ^2 soft-thresholding defined, for any dimensions N and D, $t \in \mathbb{R}^{N\times D}$, and $\rho > 0$, by

$$\mathrm{ST}_{1,2}(t, \rho)_i = \begin{cases} 0 & \text{if} \quad \|t_i\| \leqslant \rho \\ t_i - \rho\, t_i / \|t_i\| & \text{otherwise} \end{cases} \qquad \text{for all } 1 \leqslant i \leqslant N. \tag{5.8}$$

For $D = 1$, the componentwise ℓ^1-ℓ^2 soft-thresholding reduces to (3.1). Corollaries 1 and 2 can then be applied, for any $\delta_x = (\delta_f, \delta_u) \in \mathcal{X}$ and $\delta_y \in \mathcal{Y}$, using the relations

$$\begin{aligned} \partial_1\{\nabla_1 F\}(x, y, \lambda)[\delta_x] &= (\Phi^*\Phi\delta_f, 0), \\ \partial_2\{\nabla_1 F\}(x, y, \lambda)[\delta_y] &= (-\Phi^*\delta_y, 0), \\ \partial_3\{\nabla_1 F\}(x, y, \lambda) &= (0, 0), \\ \partial_1\{\mathrm{Prox}_{\tau G_1}\}(x, y, \lambda)[\delta_x] &= (\delta_f, \partial_1 \mathrm{ST}_{1,2}(u, \tau\lambda)[\delta_u]), \\ \partial_2\{\mathrm{Prox}_{\tau G_1}\}(x, y, \lambda)[\delta_y] &= (0, 0), \\ \partial_3\{\mathrm{Prox}_{\tau G_1}\}(x, y, \lambda) &= (0, \partial_2 \mathrm{ST}_{1,2}(u, \tau\lambda)), \\ \partial_1\{\mathrm{Prox}_{\tau G_2}\}(x, y, \lambda)[\delta_x] &= ((\mathrm{Id} + \Delta)^{-1}(\delta_f + \operatorname{div} \delta_u), \tilde{\nabla}(\mathrm{Id} + \Delta)^{-1}(\delta_f + \operatorname{div} \delta_u)), \\ \partial_2\{\mathrm{Prox}_{\tau G_2}\}(x, y, \lambda)[\delta_y] &= (0, 0), \\ \partial_3\{\mathrm{Prox}_{\tau G_2}\}(x, y, \lambda) &= (0, 0), \end{aligned}$$

where the weak derivatives of the componentwise ℓ^1-ℓ^2 soft-thresholding are defined, for any dimensions N and D, $t \in \mathbb{R}^{N\times D}$, $\rho > 0$, and $\delta_t \in \mathbb{R}^{N\times D}$, by

$$\partial_1 \mathrm{ST}_{1,2}(t, \rho)[\delta_t]_i = \begin{cases} 0 & \text{if} \quad \|t_i\| \leqslant \rho, \\ \delta_{t,i} - \frac{\rho}{\|t_i\|} P_{t_i}(\delta_{t,i}) & \text{otherwise}, \end{cases} \tag{5.9}$$

$$\partial_2 \mathrm{ST}_{1,2}(t, \rho)_i = \begin{cases} 0 & \text{if} \quad \|t_i\| \leqslant \rho, \\ -t_i / \|t_i\| & \text{otherwise}, \end{cases}$$

where P_α is the orthogonal projector on $\alpha^\perp$ for $\alpha \in \mathbb{R}^2$.

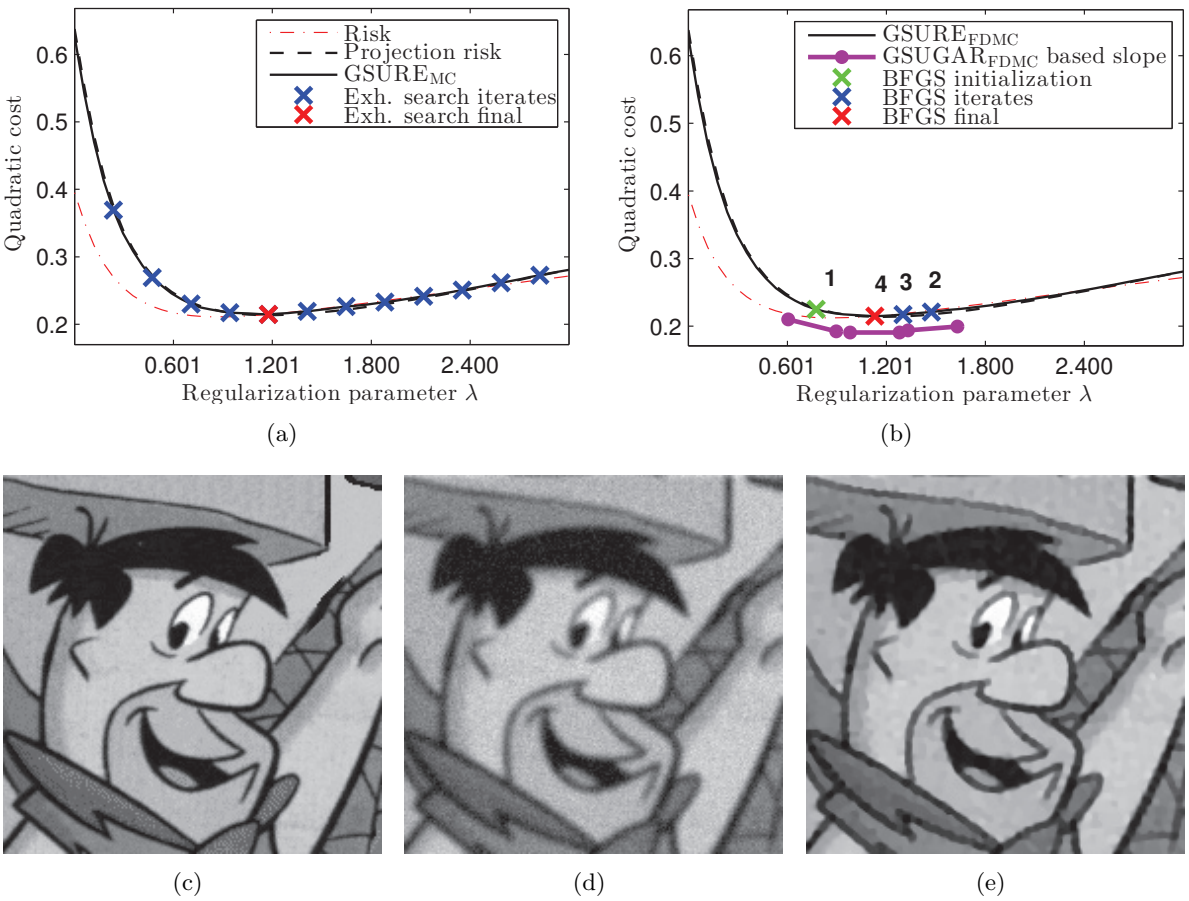

Figure 5. (a)–(b) *Risk, projection risk, and the* GSURE *estimates*[7] *as functions of the regularization parameter* λ. (a) *The* 12 *points where* $\mathrm{GSURE}_{\mathrm{MC}}\{x\}(y,\lambda,\delta)$ *has been evaluated by exhaustive search.* (b) *The four evaluation points of* $\mathrm{GSURE}_{\mathrm{FDMC}}\{x\}(y,\lambda,\delta,\varepsilon)$ *and* $\mathrm{GSUGAR}_{\mathrm{FDMC}}\{x\}(y,\lambda,\delta,\varepsilon)$ *required by BFGS to reach the optimal* λ. (c)–(e) *Respectively, a zoom-in of the underlying image* x_0*, the observation* y*, and the solution* $x(y,\lambda)$ *at the optimal* λ.

Application to image deblurring. We illustrate the total variation regularization on an image deblurring problem. We therefore consider the forward model $Y = \Phi x_0 + W \in \mathbb{R}^P$, $W \sim \mathcal{N}(0, \sigma^2 \mathrm{Id}_P)$, where x_0 is a piecewise constant (or approximately so) image and Φ is a discrete convolution matrix.

We have taken a cartoon-like image of size $(n_1, n_2) = (512, 512)$ and $P = 512^2$ observations corresponding to noisy observations of a convolution product with a discrete Gaussian kernel of radius 2 pixels. To ensure numerical stability of the pseudoinverse (typically for the least-squares estimate and the computation of the projection risk and its estimate), the kernel has been truncated in the Fourier domain such that too small contributions have been set to 0. The consequence is that around 80% of (high) frequencies are masked. The standard deviation of the noise has been set to $\sigma = 10$ (for an image x_0 with a range $[0, 255]$) such that the resulting minimum least-squares estimate $x_{\mathrm{LS}}(y) = \Phi^+ y$ has a peak signal-to-noise ratio

(PSNR) equal to $10\log_{10}(255^2/\|x_{\mathrm{LS}}(y)-x_0\|_F^2)=21.02$ dB.

Figures 5(a) and 5(b) display the risk, the projection risk, and the GSURE $=$ SURE^A (with $A=\Pi$) estimates as a function of λ obtained from a single realization of y and δ. In Figure 5(a), $\mathrm{GSURE}_{\mathrm{MC}}\{x\}(y,\lambda,\delta)$ has been evaluated for 12 values of λ chosen in a suitable tested range using the algorithm given in Figure 2. Figure 5(b) shows the benefit of computing $\mathrm{GSURE}_{\mathrm{FDMC}}\{x\}(y,\lambda,\delta,\varepsilon)$ and $\mathrm{GSUGAR}_{\mathrm{FDMC}}\{x\}(y,\lambda,\delta,\varepsilon)$, as described in Figure 3, to realize a quasi-Newton optimization. The sequence of iterates λ_n is represented, as well as the sequence of the slopes of $\mathrm{GSURE}_{\mathrm{FDMC}}\{x\}(y,\lambda_n,\delta,\varepsilon)$ given by $\mathrm{GSUGAR}_{\mathrm{FDMC}}\{x\}(y,\lambda_n,\delta,\varepsilon)$. The BFGS algorithm reaches the optimal value in only four iterations. The deviation of $\mathrm{GSURE}_{\mathrm{FDMC}}\{x\}(y,\lambda,\delta,\varepsilon)$ from the projection risk is of the same order as the deviation of $\mathrm{GSURE}_{\mathrm{MC}}\{x\}(y,\lambda,\delta)$. At the optimum value $\lambda^\star$ minimizing the GSURE, the true risk is not too far from its minimum, showing that, relative to the range of variation of the risk, in this case, the projection risk is indeed a good objective in order to minimize the risk. In Figures 5(c)–5(e), the solution $x(y,\lambda^\star)$ is compared to x_0 and y. The solution $x(y,\lambda^\star)$ has a PSNR of 24.98 dB (i.e., a gain of about 3.94 dB). Remark that, given such a noise level and convolution operator, masking 80% of (high) frequencies, the solution selected by minimizing the GSURE criterion is still a bit blurred and exhibits a staircasing effect. Using a larger regularization parameter λ would result in a more "cartoon"-like result with less blur. This would, however, entail a larger bias, which corresponds to a loss of contrast inherent to the convexity of the TV prior. This larger bias subsequently would degrade the MSE, which explains why it is not selected by the GSURE criterion.

5.4. Weighted ℓ_1-analysis wavelet regularization. We focus on the recovery of a piecewise regular image $x_0\in\mathbb{R}^{n_1\times n_2}$ from an observation y of $Y=\Phi x_0+W\in\mathbb{R}^P$, $W\sim\mathcal{N}(0,\sigma^2\mathrm{Id}_P)$, using a J-scale undecimated wavelet analysis regularization of the form

$$x^\star(y,\lambda)\in\operatorname*{Argmin}_x \frac{1}{2}\|\Phi x-y\|^2+\|\Psi x\|_{1,\lambda}, \quad \text{where} \quad \Psi=\begin{pmatrix}\Psi_1^h\\ \Psi_1^v\\ \vdots\\ \Psi_J^h\\ \Psi_J^v\end{pmatrix} \tag{5.10}$$

and λ is a vector of $\mathbb{R}^{+J}$ and $\Psi\in\mathbb{R}^{2JN\times N}$ is the analysis operator of a two-orientation wavelet transform, where, for all scales $1\leqslant j\leqslant J$, Ψ_j^h, Ψ_j^v are defined such that, for $x\in\mathbb{R}^N$, $u_j^h=\Psi_j^h x$ and $u_j^v=\Psi_j^v x$ are the vectors of undecimated wavelet coefficients of x in the horizontal and vertical directions, respectively, at the decomposition level j. The weighted ℓ^1-norm $\|.\|_{1,\lambda}$ is

$$\|\Psi x\|_{1,\lambda}=\sum_{j=1}^{J}\lambda_j\left(\left\|\Psi_j^h x\right\|_1+\left\|\Psi_j^v x\right\|_1\right).$$

Multiscale wavelet analysis promotes piecewise regular images by enforcing smoothness while preserving sharp discontinuities at different scales and orientations. Each parameter λ_j controls the regularity at scale j. A large value of λ_j tends to oversmooth structures at scale j, while a small value leads to undersmoothing. As noted in several papers (see, e.g., [11, 49]), the

optimal values λ_j are also image- and degradation-dependent, revealing again the importance of automatic selection procedures.

Problem (5.10) is a special instance of (4.3) where the parameter $\lambda = \theta \in \Theta = \mathbb{R}^{+J}$ and

$$\begin{aligned} H(x,y,\lambda) &= \tfrac{1}{2}\|\Phi x - y\|^2, \\ G(u,y,\lambda) &= \|u\|_{1,\lambda}, \\ K(x) &= \Psi x. \end{aligned}$$

Hence the primal-dual CP splitting can be used to solve (5.10) using

$$\begin{aligned} \mathrm{Prox}_{\xi H}(x,y,\lambda) &= x + \xi\Phi^* y - \xi\Phi^*(\mathrm{Id} + \xi\Phi\Phi^*)^{-1}\Phi(x + \xi\Phi^* y), \\ \mathrm{Prox}_{\tau G^*}(u,y,\lambda) &= u - \tau \mathrm{ST}(u/\tau, \lambda/\tau), \\ K^*(u,\lambda) &= \sum_{j=1}^{J} (\Psi_j^{h*} u_j^h + \Psi_j^{v*} u_j^v), \end{aligned}$$

where ST denotes in this section the multiscale extension of the soft-thresholding operator (3.1) such that, for $t \in \mathbb{R}^{2JN}$ and $\rho \in \mathbb{R}^J$, we have

$$\mathrm{ST}(t,\rho)_j^o = \mathrm{ST}(t_j^o, \rho_j)$$

for all scales $1 \leqslant j \leqslant J$ and orientations $o = v, h$. Corollaries 1 and 2 can then be applied using

$$\begin{aligned} \partial_1\{\mathrm{Prox}_{\xi H}\}(x,y,\lambda)[\delta_x] &= \delta_x + \xi\Phi^*(\mathrm{Id} + \xi\Phi\Phi^*)^{-1}\Phi\delta_x, \\ \partial_2\{\mathrm{Prox}_{\xi H}\}(x,y,\lambda)[\delta_y] &= \xi\Phi^*\delta_y - \xi^2\Phi^*(\mathrm{Id} + \xi\Phi\Phi^*)^{-1}\Phi\Phi^*\delta_y, \\ \partial_3\{\mathrm{Prox}_{\xi H}\}(x,y,\lambda) &= 0, \\ \partial_1\{\mathrm{Prox}_{\tau G^*}\}(u,y,\lambda)[\delta_u] &= \delta_u - \partial_1 \mathrm{ST}(u/\tau, \lambda/\tau)[\delta_u], \\ \partial_2\{\mathrm{Prox}_{\tau G^*}\}(u,y,\lambda)[\delta_y] &= 0, \\ \partial_3\{\mathrm{Prox}_{\tau G^*}\}(u,y,\lambda) &= -\partial_2 \mathrm{ST}(u/\tau, \lambda/\tau), \end{aligned}$$

where the derivatives of the multiscale soft-thresholding are defined, for any $t \in \mathbb{R}^{2JN}$, $\rho \in \mathbb{R}^J$, and $\delta_t \in \mathbb{R}^{2JN}$, by

$$\partial_1 \mathrm{ST}(t,\rho)[\delta_t]_j^o = \partial_1 \mathrm{ST}(t_j^o, \rho_j)[\delta_{t_j}^o] \quad \text{and} \quad \partial_2 \mathrm{ST}(t,\rho)_j^o = \partial_2 \mathrm{ST}(t_j^o, \rho_j) \tag{5.11}$$

for all scales $1 \leqslant j \leqslant J$ and orientations $o = v, h$.

Application to compressed sensing. We illustrate the multiscale wavelet ℓ_1-analysis regularization on a compressed sensing problem. We therefore consider the forward model $Y = \Phi x_0 + W \in \mathbb{R}^P$, $W \sim \mathcal{N}(0, \sigma^2 \mathrm{Id}_P)$, where x_0 is a piecewise multiscale regular (or approximately so) image and Φ is a random matrix. Here the multiscale transform W is constructed from undecimated Daubechies 4 wavelets [15].

We have taken a uniformly randomized subsampling of a uniform random convolution, where $(P/N = 0.5)$. The standard deviation has been set to $\sigma = 10$ (for an image x_0 with a range $[0, 255]$) such that the resulting minimum least-squares estimate $x_{\mathrm{LS}}(y) = \Phi^+ y$ has a PSNR given by $10 \log_{10}(255^2 / \|x_{\mathrm{LS}}(y) - x_0\|_F^2) \approx 16$ dB.

Table 1

Illustration of the minimization of $\mathrm{SURE}_{\mathrm{FDMC}}$ *in multiscale regularization obtained for the three images in Figure 6 with different numbers of scales from* $J = 1$ *to* $J = 3$ *using either one global parameter or one parameter per scale. For each case, the obtained optimal parameters* $\lambda^\star$ *are given. The associated value of* SURE *and the PSNR are compared to neighbors of* $\lambda^\star$ *located at* $0.75\lambda^\star$ *and* $1.25\lambda^\star$*. Boldface numbers are used to indicate for each criterion the best sets of parameters.*

Input		Optimal parameters			SURE/PSNR		
Image	PSNR	J	$\dim \Lambda$	$\lambda^\star$	$0.75\lambda^\star$	$\lambda^\star$	$1.25\lambda^\star$
`Mandrill`	17.37	1	1	(7.58)	7.53/24.84	**7.39**/24.90	7.43/**24.94**
		2	1	(5.63)	7.60/24.85	**7.45**/24.88	7.58/**24.89**
		3	1	(4.54)	7.87/24.04	**7.71**/**24.10**	7.83/**24.10**
		2	2	(5.94, 4.24)	7.49/25.02	**7.30**/25.06	7.38/**25.07**
		3	3	(7.51, 1.07, 0.99)	7.37/25.12	**7.22**/25.18	7.33/**25.20**
`House`	17.65	1	1	(18.38)	3.69/**31.16**	**3.51**/31.15	3.68/30.55
		2	1	(11.11)	3.72/31.31	**3.51**/**31.40**	3.81/31.05
		3	1	(8.73)	4.30/30.18	**4.08**/**30.31**	4.43/30.13
		2	2	(14.47, 5.20)	3.53/31.51	**3.34**/**31.57**	3.55/31.05
		3	3	(15.00, 2.50, 2.83)	3.52/31.55	**3.27**/**31.63**	3.44/31.14
`Cameraman`	15.13	1	1	(13.50)	5.29/28.61	**5.09**/**28.73**	5.35/28.64
		2	1	(8.78)	5.34/28.75	**5.09**/**28.83**	5.38/28.72
		3	1	(7.14)	5.84/28.03	**5.60**/**28.06**	5.88/27.99
		2	2	(10.98, 3.74)	5.16/28.91	**4.90**/**29.04**	5.09/28.96
		3	3	(11.56, 3.31, 0.97)	5.07/29.00	**4.86**/**29.11**	5.13/28.99

Table 1 and Figure 6 illustrate the multiscale regularization obtained by minimizing the $\mathrm{SURE} = \mathrm{SURE}^A$ (with $A = \mathrm{Id}$) for three different images x_0, known as `Mandrill`, `House`, and `Cameraman`, and a single realization of y and δ. Three levels of decomposition from $J = 1$ to $J = 3$ are considered. We also consider using either one global regularization parameter or one parameter per scale. Table 1 gives the selected optimal vector of parameters $\lambda^\star$ for each level of decomposition and their associated performance in terms of SURE and PSNR. We first observe that, compared to the global approach, optimizing one parameter per scale indeed adapts better to the regularity of the image. For instance, the image `Mandrill` contains fine scales with more energy than `House`; then the obtained penalization of the first scale is smaller for `Mandrill` than for `House`. Visual inspection of these results in Figure 6 illustrates this automatic adaptation. In the same vein, with three levels of decomposition, the penalization is less severe for `Mandrill` than for `House` and `Cameraman`. We next observe that increasing the level of decomposition improves the PSNR when using one parameter per scale, while this is not the case when a global parameter is used. The gap is more important between $J = 1$ and $J = 2$. To assess the minimization of $\mathrm{SURE}_{\mathrm{FDMC}}$, we have compared the SURE and the PSNR values at $0.75\lambda^\star$ and $1.25\lambda^\star$. At the optimal $\lambda^\star$, the SURE is, as expected, minimal. Furthermore, at $\lambda^\star$, the PSNR is either maximal or not too far from its maximal value, showing that, in this case, the prediction risk is indeed a good objective in order to maximize the PSNR.

6. Conclusion.

We have proposed a methodology for optimizing multiple continuous parameters of a weakly differentiable estimator that attempts to solve a linear ill-posed inverse problem contaminated by additive white Gaussian noise. The proposed method selects the parameters that minimize an estimate of the risk and is driven by an estimate of its gradi-

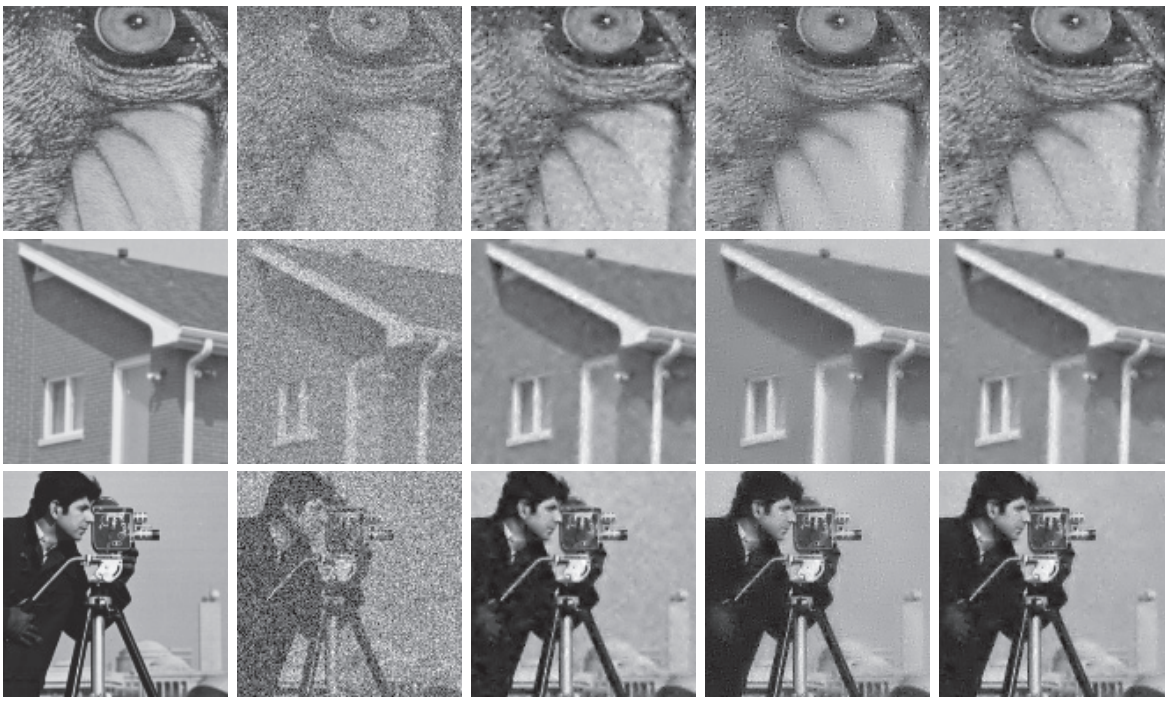

(a) (b) (c) (d) (e)

Figure 6. *From top to bottom, a close-up of* `Mandrill`*,* `House`*, and* `Cameraman`*.* (a) *Underlying image* x_0. (b) *Least-squares estimate* $x_{\mathrm{LS}}(y)$. (c) *Result with* $\lambda^\star$ *for one level of decomposition* $J = 1$, (d) *for three levels of decomposition* $J = 3$ *using one global parameter, and* (e) *for three levels of decomposition* $J = 3$ *using one parameter per scale.*

ent. Classical unbiased estimators of the risk are generally noncontinuous functions of the parameters, so that their local variations cannot be used to estimate the gradient of the risk. These estimators require estimating the DOF by evaluating the variations of the estimator with respect to the observations. We have shown that estimating the DOF by finite differences leads to a weakly differentiable risk estimator. By carefully choosing the finite-difference step and by computing explicitly the (weak) gradient of this estimate, an asymptotically unbiased estimator of the gradient of the risk is obtained. This estimator is numerically smooth enough to apply a quasi-Newton method. An explicit strategy for computing this (weak) gradient is given for a large class of (iterative) weakly differentiable algorithms. We exemplified our methodology on several popular proximal splitting methods. Numerical experiments demonstrated the wide applicability and scope of the approach.

Our choice of the finite-difference step size was essentially guided by a careful analysis of the soft-thresholding estimator. Choosing this step size with theoretical guarantees (such as consistency or optimality) in more general cases remains an open question. Beyond consistency and optimality, the question of quantifying the influence of the finite-difference step on the smoothness of the risk gradient estimates and then on the performance of quasi-Newton methods is still open. To deal with parameter space of higher dimensions, other Jacobian accumulation strategies could be explored following [35]. Improvements could also be achieved on the settings of the quasi-Newton methods. In particular, a drawback of our approach is

the sensitivity to local minima of the risk with respect to the collection of parameters. In some settings, more elaborate optimization strategies could be employed. Future work could also focus on the extensions to nonweakly differentiable estimators and/or inverse problems with non-Gaussian noises.

Appendix A. Proofs of section 3.

Proof of Proposition 1. This is a consequence of the chain rule and linearity of the weak derivative. Indeed, $\widehat{df}^A_{\mathrm{FD}}\{\mu\}(y,\theta,\varepsilon)$ is just the sum of P weakly differentiable functions and hence is weakly differentiable with the weak derivative with respect to θ as given. Moreover, $\|A(\mu(y,\theta)-y)\|^2 = \sum_{i=1}^P \left((A(\mu(y,\theta)-y))_i\right)^2$. Each term i is the composition of a weakly differentiable function $(A(\mu(y,\cdot)-y))_i$ and $(\cdot)^2$, where the latter is obviously continuously differentiable with bounded derivative and takes 0 at the origin. It then follows from the chain rule [29, Theorem 4(ii), section 4.2.2] that $(A(\mu(y,\cdot)-y))_i$ is weakly differentiable, and the weak derivative of $\|A(\mu(y,\cdot)-y)\|^2$ with respect to θ is indeed

$$2\partial_2\mu(y,\theta)^* A^* A(\mu(y,\theta)-y). \qquad \blacksquare$$

Proof of Theorem 1. The proof strategy consists in commuting in an appropriate order the different signs (limit, integration, and derivation) while checking that our assumptions provide sufficient conditions for this to hold.

Let V be a compact subset of Θ, and choose $\varphi \in C^1_c(\Theta)$ with support in V. We have

$$\begin{aligned}
\int_\Theta R^A\{\mu\}(\mu_0,\theta)\frac{\partial\varphi(\theta)}{\partial\theta_i}d\theta &= \int_V R^A\{\mu\}(\mu_0,\theta)\frac{\partial\varphi(\theta)}{\partial\theta_i}d\theta \\
&= \int_V \mathbb{E}_W\left[\|A(\mu(Y,\theta)-y)\|^2\right]\frac{\partial\varphi(\theta)}{\partial\theta_i}d\theta \\
\text{[Stein lemma]} &\overset{(S.1)}{=} \int_V \mathbb{E}_W\left[\mathrm{SURE}^A\{\mu\}(Y,\theta)\right]\frac{\partial\varphi(\theta)}{\partial\theta_i}d\theta \\
\text{[(2.8)]} &\overset{(S.2)}{=} \int_V \mathbb{E}_W\left[\lim_{\varepsilon\to0}\mathrm{SURE}^A_{\mathrm{FD}}\{\mu\}(Y,\theta,\varepsilon)\right]\frac{\partial\varphi(\theta)}{\partial\theta_i}d\theta \\
\text{[dominated convergence]} &\overset{(S.3)}{=} \lim_{\varepsilon\to0}\int_V \mathbb{E}_W\left[\mathrm{SURE}^A_{\mathrm{FD}}\{\mu\}(Y,\theta,\varepsilon)\right]\frac{\partial\varphi(\theta)}{\partial\theta_i}d\theta \\
\text{[Fubini]} &\overset{(S.4)}{=} \lim_{\varepsilon\to0}\mathbb{E}_W\left[\int_V \mathrm{SURE}^A_{\mathrm{FD}}\{\mu\}(Y,\theta,\varepsilon)\frac{\partial\varphi(\theta)}{\partial\theta_i}d\theta\right] \\
\text{[weak differentiability, Proposition 1]} &\overset{(S.5)}{=} -\lim_{\varepsilon\to0}\mathbb{E}_W\left[\int_V \frac{\partial}{\partial\theta_i}\mathrm{SURE}^A_{\mathrm{FD}}\{\mu\}(Y,\theta,\varepsilon)\varphi(\theta)d\theta\right] \\
\text{[Proposition 1]} &\overset{(S.6)}{=} -\lim_{\varepsilon\to0}\mathbb{E}_W\left[\int_V \left(\mathrm{SUGAR}^A_{\mathrm{FD}}\{\mu\}(Y,\theta,\varepsilon)\right)_i\varphi(\theta)d\theta\right] \\
\text{[Fubini]} &\overset{(S.7)}{=} -\lim_{\varepsilon\to0}\int_V \mathbb{E}_W\left[\left(\mathrm{SUGAR}^A_{\mathrm{FD}}\{\mu\}(Y,\theta,\varepsilon)\right)_i\right]\varphi(\theta)d\theta \\
\text{[dominated convergence]} &\overset{(S.8)}{=} -\int_V\left(\lim_{\varepsilon\to0}\mathbb{E}_W\left[\left(\mathrm{SUGAR}^A_{\mathrm{FD}}\{\mu\}(Y,\theta,\varepsilon)\right)_i\right]\right)\varphi(\theta)d\theta \\
&= -\int_\Theta\left(\lim_{\varepsilon\to0}\mathbb{E}_W\left[\left(\mathrm{SUGAR}^A_{\mathrm{FD}}\{\mu\}(Y,\theta,\varepsilon)\right)_i\right]\right)\varphi(\theta)d\theta.
\end{aligned}$$

From the definition of weak derivative, we get the claimed result on the asymptotic unbiasedness of $\mathrm{SUGAR}^A_{\mathrm{FD}}$. The asymptotic unbiasedness of the gradient of the finite-difference DOF naturally follows with the same proof strategy by ignoring the two first terms in the decomposition $\mathrm{SURE}^A_{\mathrm{FD}}\{\mu\}(\mu_0,\theta,\varepsilon) = \|A(\mu(y,\theta)-y)\|^2 - \sigma^2\operatorname{tr}(A^*A) + 2\sigma^2\widehat{df}^A_{\mathrm{FD}}\{\mu\}(\mu_0,\theta,\varepsilon)$.

We now justify each of the above steps (S.1)–(S.8). We denote by $g_{1,\sigma}$ the Gaussian probability density function of zero mean and variance σ^2, and by g_σ its P-dimensional version, i.e., $g_\sigma = (g_{1,\sigma})^P$.

(S.1) This is the Stein lemma, which applies owing to assumption (A1). Indeed, $\mu(\cdot,\theta)$ is Lipschitz, and hence weakly differentiable, and its derivative equals its weak derivative Lebesgue-a.e. [29, Theorems 1–2, section 6.2]. Moreover, we have for any θ

$$\|\mu(y,\theta)-\mu(y',\theta)\| \leqslant L_1\|y-y'\| \Rightarrow |\mu_i(y,\theta)-\mu_i(y',\theta)| \leqslant L_1\|y-y'\|, \tag{A.1}$$

and thus, whenever the derivatives of $\mu_i(\cdot,\theta)$ exist, they are bounded by L_1. Consequently,

$$\mathbb{E}_W\left[\left|\frac{\partial\mu_i(Y)}{\partial y_i}\right|\right] \leqslant L_1;$$

i.e., the weak partial derivatives are essentially bounded.

(S.2) This step is just (2.8) with the arguments justifying it owing to assumption (A1).

(S.3) Let $f_\varepsilon(y,\theta) = \mathrm{SURE}^A_{\mathrm{FD}}\{\mu\}(y,\theta,\varepsilon)$. From (2.8), $\lim_{\varepsilon\to 0} f_\varepsilon(y,\theta) = \mathrm{SURE}^A\{\mu\}(y,\theta)$ exists Lebesgue-a.e. Assumptions (A1)–(A2) give

$$\|\mu(y,\theta)-y\| \leqslant \|y\| + \|\mu(y,\theta)-\mu(0,\theta)\| \leqslant (1+L_1)\|y\|.$$

Combining this with (A.1) leads to

$$\begin{aligned}|f_\varepsilon(y,\theta)| &= \left|\|A(\mu(y,\theta)-y)\|^2 - \sigma^2\operatorname{tr}(A^*A) + 2\sigma^2\frac{1}{\varepsilon}\sum_{i=1}^P (A^*A(\mu(y+\varepsilon e_i,\theta)-\mu(y,\theta)))_i\right| \\ &\leqslant \|A\|^2 P\sigma^2\left((1+L_1)^2\frac{\|y\|^2}{P\sigma^2}+1+2L_1\right).\end{aligned}$$

Note that the bound is independent of θ. Thus

$$\begin{aligned}&\mathbb{E}_W\left[\|A\|^2 P\sigma^2\left((1+L_1)^2\frac{\|y\|^2}{P\sigma^2}+1+2L_1\right)\right] \\ &\qquad = \|A\|^2 P\sigma^2\left((1+L_1)^2\left(\frac{\|\mu_0\|^2}{P\sigma^2}+1\right)+1+2L_1\right) < \infty.\end{aligned}$$

This bound together with the fact that φ is continuously differentiable with compact support in V means that $f_\varepsilon\frac{\partial\varphi}{\partial\theta_i}$ is dominated by an integrable function on $\mathcal{Y}\times V$. The dominated convergence then applies, which yields the claim.

(S.4) The Fubini theorem surely applies in view of the integrability just shown at the end of (S.3).

(S.5) This is a consequence of Proposition 1 and the definition of weak differentiability since $\mu(y,\cdot)$ is Lipschitz continuous independently of y.

(S.6) This step holds by definition of $\mathrm{SUGAR}^{A}_{\mathrm{FD}}\{\mu\}$ in Proposition 1.

(S.7) Let $f_\varepsilon(y,\theta) = (\mathrm{SUGAR}^{A}_{\mathrm{FD}}\{\mu\}(y,\theta,\varepsilon))_i$ and $h(y,\theta) = (2\partial_2\mu(y,\theta)^* A^*A(\mu(y,\theta)-y))_i$. By the translation invariance of the convolution product, we have

$$\mathbb{E}_W[f_\varepsilon(Y,\theta)] = 2(g_\sigma * h(\cdot,\theta))(\mu_0) + 2\sigma^2 \sum_{j=1}^{P} \frac{g_\sigma(\cdot+\varepsilon e_i) - g_\sigma}{\varepsilon} * \left(\partial_2\mu(\cdot,\theta)^* A^* A e_j\right)_i (\mu_0).$$

Thus

$$\begin{aligned}
|(g_\sigma * h(\cdot,\theta))(\mu_0)| &\leqslant 2\int_{\mathcal{Y}} g_\sigma(y-\mu_0)\,|(\partial_2\mu(y,\theta)^* A^*A(\mu(y,\theta)-y))_i|\,dy \\
\text{[assumption (A3)]} &\leqslant 2L_2\,\|A\|^2 \int_{\mathcal{Y}} g_\sigma(y-\mu_0)\,\|\mu(y,\theta)-y\|\,dy \\
\text{[assumptions (A1)–(A2)]} &\leqslant 2(1+L_1)L_2\,\|A\|^2 \int_{\mathcal{Y}} g_\sigma(y-\mu_0)\,\|y\|\,dy \\
&\leqslant 2(1+L_1)L_2\,\|A\|^2\,\mathbb{E}_W[\|y\|]dy \\
\text{[Jensen inequality]} &\leqslant 2(1+L_1)L_2\,\|A\|^2\,\mathbb{E}_W[\|y\|^2]^{1/2}dy \\
&\leqslant 2(1+L_1)L_2\,\|A\|^2 \left(\|\mu_0\|^2 + P\sigma^2\right)^{1/2} < \infty.
\end{aligned}$$

For the second term, we have

$$\begin{aligned}
&\left|\frac{g_\sigma(\cdot+\varepsilon e_i) - g_\sigma}{\varepsilon} * \left(\partial_2\mu(\cdot,\theta)^* A^* A e_j\right)_i (\mu_0)\right| \\
&\leqslant \int_{\mathcal{Y}} \left|\frac{g_\sigma(y-\mu_0+\varepsilon e_i) - g_\sigma(y-\mu_0)}{\varepsilon}\right| \left|(\partial_2\mu(y,\theta)^* A^* A e_j)_i\right| dy \\
\text{[assumption (A3)]} &\leqslant L_2\,\|A\|^2 \int_{\mathcal{Y}} \left|\frac{g_\sigma(y-\mu_0+\varepsilon e_i) - g_\sigma(y-\mu_0)}{\varepsilon}\right| dy \\
&\leqslant L_2\,\|A\|^2 \int_{\mathbb{R}} \left|\frac{g_{1,\sigma}(t-(\mu_0)_i+\varepsilon) - g_{1,\sigma}(t-(\mu_0)_i)}{\varepsilon}\right| dt \\
\text{[Taylor]} &\leqslant L_2\,\|A\|^2 \int_{\mathbb{R}} \int_0^1 \left|g'_{1,\sigma}(t-(\mu_0)_i+\tau)\right| dt d\tau \\
\text{[Fubini]} &\leqslant L_2\,\|A\|^2 \int_{\mathbb{R}} \left|g'_{1,\sigma}(t)\right| dt < \infty.
\end{aligned}$$

In view of these bounds, and since φ is compactly supported in V, integrability of $f_\varepsilon\varphi$ on $\mathcal{Y}\times V$ is ensured, whence the claimed result follows.

(S.8) Let f_ε be defined as in step (S.7). We have just shown that the integrand in θ, i.e., $\mathbb{E}_W[f_\varepsilon(Y,\cdot))_i]\varphi$, is dominated by a function that is integrable on V. It remains to check that its limit exists Lebesgue-a.e. But this is yet again an application of the dominated convergence theorem to the sequence f_ε as an integrand with respect to the Gaussian measure $g_\sigma(y)dy$, which allows us to deduce that $\lim_{\varepsilon\to 0}\mathbb{E}_W[f_\varepsilon(Y,\theta)\varphi(\theta)] = \mathbb{E}_W[\lim_{\varepsilon\to 0} f_\varepsilon(Y,\theta)\varphi(\theta)]$.

This completes the proof. ■

Proof of Proposition 1. For a fixed λ, it can be shown similarly to [29, Theorem 4(iii), section 4.2.2] that $\mathrm{ST}(\cdot,\lambda)$ is weakly differentiable and that its weak Jacobian $h(y)=\partial_2\mathrm{ST}(y,\lambda)$ is diagonal, with diagonal elements, for $1\leqslant i\leqslant P$,

$$h(y)_i=\begin{cases}+1 & \text{if} \quad y_i\leqslant-\lambda,\\ 0 & \text{if} \quad -\lambda<y_i<\lambda,\\ -1 & \text{otherwise.}\end{cases} \tag{A.2}$$

We next define, for a fixed λ, the quantity $h'(y,\varepsilon)=\nabla_2\{\widehat{df}_{\mathrm{FD}}\{\mathrm{ST}\}\}(y,\lambda,\varepsilon)$. Using Proposition 1 and the fact that $\varepsilon<2\lambda$ gives

$$h'(y,\varepsilon)=\sum_{i=1}^{P}\frac{h(y+\varepsilon e_i)_i-h(y)_i}{\varepsilon}=\sum_{i=1}^{P}\begin{cases}0 & \text{if} \quad y_i<-\lambda-\varepsilon,\\ -1/\varepsilon & \text{if} \quad -\lambda-\varepsilon<y_i<-\lambda,\\ 0 & \text{if} \quad -\lambda<y_i<\lambda-\varepsilon,\\ -1/\varepsilon & \text{if} \quad \lambda-\varepsilon<y_i<\lambda,\\ 0 & \text{if} \quad \lambda<y_i.\end{cases}$$

Computing the expectation and the variance of $h'(Y,\varepsilon)$ in closed form with truncated Gaussian statistics and using the fact that h is separable in its arguments give the proposed formula. ■

Proof of Theorem 2. For P big enough, $\hat{\varepsilon}(P)<2\lambda$ since $\lim_{P\to\infty}\hat{\varepsilon}(P)=0$. Using the notation in the proof of Lemma 1 leads to

$$\mathrm{SUGAR}_{\mathrm{FD}}\{\mathrm{ST}\}(y,\lambda,\varepsilon)=2h(y)^*(\mathrm{ST}(y,\lambda)-y)+2\sigma^2h'(y,\hat{\varepsilon}(P)).$$

The Cauchy–Schwarz inequality implies that

$$\begin{aligned}\mathbb{V}_W\left[\frac{1}{P}\mathrm{SUGAR}_{\mathrm{FD}}\{\mathrm{ST}\}(Y,\lambda,\varepsilon)\right]^{1/2}\leqslant{}&2\mathbb{V}_W\left[\frac{1}{P}h(y)^*(\mathrm{ST}(Y,\lambda)-Y)\right]^{1/2}\\&+2\sigma^2\mathbb{V}_W\left[\frac{1}{P}h'(Y,\hat{\varepsilon}(P))\right]^{1/2}.\end{aligned}$$

Since $x\mapsto\sqrt{\pi}\,\mathrm{erf}\,(x/a)$ is Lipschitz continuous with a constant of $2/a$, Lemma 1 yields

$$\mathbb{V}_W\left[\frac{1}{P}h'(Y,\hat{\varepsilon}(P))\right]\leqslant\frac{\sqrt{2}}{\sqrt{\pi}\sigma P\hat{\varepsilon}(P)}.$$

By assumption, we have $\lim_{P\to\infty}P^{-1}\hat{\varepsilon}(P)^{-1}=0$, and then the variance of $\frac{1}{P}h'(Y,\hat{\varepsilon}(P))$ vanishes to zero. Next, remark that

$$h(y)^*(\mathrm{ST}(y,\lambda)-y)=\lambda\#\{|y|>\lambda\},$$

where $\#\{|y|>\lambda\}$ denotes the number of entries of $|y|$ greater than λ. We have $\#\{|Y_i|>\lambda\}\sim_{\mathrm{iid}}\mathrm{Bernoulli}(p_i)$ whose variance is $p_i(1-p_i)$, where $p_i=\frac{1}{2}(\mathrm{erf}(\frac{(\mu_0)_i+\lambda}{\sqrt{2}\sigma})-\mathrm{erf}(\frac{(\mu_0)_i-\lambda}{\sqrt{2}\sigma}))$. It follows that $\mathbb{V}_W[\#\{|Y|>\lambda\}]=\sum_{i=1}^{P}p_i(1-p_i)\leqslant P$, and hence

$$\lim_{P\to\infty}\mathbb{V}_W\left[\frac{1}{P}h(Y)^*(\mathrm{ST}(Y,\lambda)-Y)\right]=\lim_{P\to\infty}\mathbb{V}_W\left[\frac{1}{P}\lambda\#\{|Y|>\lambda\}\right]=0.$$

Consistency (i.e., convergence in probability) follows from traditional arguments by invoking Chebyshev inequality and using asymptotic unbiasedness (Theorem 1) and vanishing variance. ■

Proof of Proposition 2. Developing the MSE in terms of bias and variance gives the first part of the proposition. Lemma 1 and the fact that $\lim_{\varepsilon\to 0} \mathbb{E}_W \nabla_2\{\widehat{df}\{\mathrm{ST}\}\}(Y,\lambda,\varepsilon) = \nabla_2\{df\{\mathrm{ST}\}\}(\mu_0,\lambda)$ conclude the second part. ■

Appendix B. Regularity of the proximal operator of a gauge. We first provide a glimpse of gauges.

Definition 2 (gauge). *Let $\mathcal{C}$ be a nonempty closed convex set containing the origin. The* gauge *of $\mathcal{C}$ is the function $\gamma_{\mathcal{C}}$ defined by*

$$\gamma_{\mathcal{C}}(y) = \inf\{\omega > 0 \setminus y \in \omega\mathcal{C}\}.$$

As usual, $\gamma_{\mathcal{C}}(y) = +\infty$ if the infimum is not attained.

Definition 3 (polar set). *Let $\mathcal{C}$ be a nonempty convex set. The set $\mathcal{C}^\circ$ given by*

$$\mathcal{C}^\circ = \left\{z \in \mathbb{R}^N \setminus \langle z, x\rangle \leqslant 1 \ \forall x \in \mathcal{C}\right\}$$

is called the polar *of $\mathcal{C}$. $\mathcal{C}^\circ$ is a nonempty closed convex set containing the origin, and if $\mathcal{C}$ is closed and contains the origin as well, then $\mathcal{C}^{\circ\circ} = \mathcal{C}$.*

We now summarize some key properties that will be needed in the main proof.

Lemma 2. *Let $\mathcal{C}$ be a nonempty closed convex set containing the origin. The following assertions hold.*

(i) *$\gamma_{\mathcal{C}}$ is a nonnegative closed convex and positively homogeneous function.*

(ii) *$\mathcal{C}$ is the unique closed convex set containing the origin such that*

$$\mathcal{C} = \{y \in \mathcal{Y} \setminus \gamma_{\mathcal{C}}(y) \leqslant 1\}.$$

(iii) *$\gamma_{\mathcal{C}}$ is bounded and coercive if and only if $\mathcal{C}$ is compact and contains the origin as an interior point.*

(iv) *The gauge of $\mathcal{C}$ and the support function $\sigma_{\mathcal{C}^\circ}(y) = \max_{z\in\mathcal{C}^\circ}\langle y, z\rangle$ coincide, i.e.,*

$$\gamma_{\mathcal{C}} = \sigma_{\mathcal{C}^\circ}.$$

Proof. Assertions (i)–(ii) follow from [36, Theorem V.1.2.5]. Assertion (iii) is a consequence of [36, Theorem V.1.2.5(ii) and Corollary V.1.2.6]. Assertion (iv) follows from [36, Proposition V.3.2.4]. ■

We are now equipped to prove our regularity result.

Proposition 5. *Let $\mathcal{C}$ be a compact convex set containing the origin as an interior point, i.e., a convex body, and let $G = \gamma_{\mathcal{C}}$ be its gauge. For any $\theta > 0$, $\theta' > 0$, and any $y \in \mathcal{Y}$, the following holds:*

$$\|\mathrm{Prox}_{\theta G}(y) - \mathrm{Prox}_{\theta' G}(y)\| \leqslant L_2|\theta - \theta'|$$

for some constant $L_2 > 0$ independent of y; i.e., for any y, $\theta \mapsto \mathrm{Prox}_{\theta G}(y)$ is Lipschitz continuous on $]0, +\infty[$.

Proof. From [1, Proposition 2.3(ii)], we have that for any y, the function $\theta \mapsto \mathrm{Prox}_{\theta G}(y)$ is such that

$$\|\mathrm{Prox}_{\theta G}(y) - \mathrm{Prox}_{\theta' G}(y)\| \leqslant |\theta - \theta'| \, \|y - \mathrm{Prox}_{\theta G}(y)\| \, /\theta. \tag{B.1}$$

Now, we have

$$\theta G(y) = \gamma_{\mathcal{C}/\theta}(y) = \sigma_{\theta \mathcal{C}^\circ}(y), \tag{B.2}$$

where the first equality follows from positive homogeneity (Lemma 2(i)) and Definition 2, and the second equality is a consequence of Lemma 2(iv) and polarity.

Applying Moreau's identity, we get that

$$y - \mathrm{Prox}_{\theta G}(y) = y - \mathrm{Prox}_{\sigma_{\theta \mathcal{C}^\circ}}(y) = \mathrm{Proj}_{\theta \mathcal{C}^\circ}(y).$$

By virtue of Lemma 2(iii), there exists a constant $L_2 > 0$, independent of y, such that[8]

$$\|y - \mathrm{Prox}_{\theta G}(y)\| = \|\mathrm{Proj}_{\theta \mathcal{C}^\circ}(y)\| \leqslant L_2 \gamma_{\mathcal{C}^\circ}\big(\mathrm{Proj}_{\theta \mathcal{C}^\circ}(y)\big).$$

Applying (B.2) to $\gamma_{\mathcal{C}^\circ}$, we get

$$\|y - \mathrm{Prox}_{\theta G}(y)\| \leqslant L_2 \theta \gamma_{\theta \mathcal{C}^\circ}\big(\mathrm{Proj}_{\theta \mathcal{C}^\circ}(y)\big) \leqslant L_2 \theta, \tag{B.3}$$

where the last inequality follows from Lemma 2(ii) since obviously $\mathrm{Proj}_{\theta \mathcal{C}^\circ}(y) \in \theta \mathcal{C}^\circ$. Combining (B.1) and (B.3), we get the desired result. ∎

Corollary 5. *Let $\mathcal{C}_i$, $i = 1, \ldots, m$, be compact convex sets containing the origin as an interior point, i.e., convex bodies, and let $G_i = \gamma_{\mathcal{C}_i}$ be the associated gauges. For any $\theta, \theta' \in]0, +\infty[^m$, and any $y \in \mathcal{Y}$, the following holds:*

$$\left\| \mathrm{Prox}_{\theta_1 G_1} \circ \cdots \circ \mathrm{Prox}_{\theta_m G_m}(y) - \mathrm{Prox}_{\theta'_1 G_1} \circ \cdots \circ \mathrm{Prox}_{\theta'_m G_m}(y) \right\| \leqslant \sqrt{m} \max_i L_{2,i} \left\| \theta - \theta' \right\|,$$

where $L_{2,i} > 0$ is the same Lipschitz constant associated to $\mathcal{C}_i$ given in Proposition 5.

Proof. Using repeatedly the triangle inequality, Proposition 5, and the fact that the mapping $y \mapsto \mathrm{Prox}_{\theta_i G_i}(y)$ is 1-Lipschitz [57], we obtain

$$\begin{aligned}
&\left\| \mathrm{Prox}_{\theta_1 G_1} \circ \cdots \circ \mathrm{Prox}_{\theta_m G_m}(y) - \mathrm{Prox}_{\theta'_1 G_1} \circ \cdots \circ \mathrm{Prox}_{\theta'_m G_m}(y) \right\| \\
&= \Big\| \Big(\mathrm{Prox}_{\theta_1 G_1} \circ \mathrm{Prox}_{\theta_2 G_2} \circ \cdots \circ \mathrm{Prox}_{\theta_m G_m}(y) - \mathrm{Prox}_{\theta'_1 G_1} \circ \mathrm{Prox}_{\theta_2 G_2} \circ \cdots \circ \mathrm{Prox}_{\theta_m G_m}(y) \Big) \\
&\quad + \Big(\mathrm{Prox}_{\theta'_1 G_1} \circ \mathrm{Prox}_{\theta_2 G_2} \circ \cdots \circ \mathrm{Prox}_{\theta_m G_m}(y) - \mathrm{Prox}_{\theta'_1 G_1} \circ \mathrm{Prox}_{\theta'_2 G_2} \circ \cdots \circ \mathrm{Prox}_{\theta_m G_m}(y) \Big) \Big\| \\
&\leqslant L_{2,1} |\theta_1 - \theta'_1| + \left\| \mathrm{Prox}_{\theta_2 G_2} \circ \cdots \circ \mathrm{Prox}_{\theta_m G_m}(y) - \mathrm{Prox}_{\theta'_2 G_2} \circ \cdots \circ \mathrm{Prox}_{\theta'_m G_m}(y) \right\| \\
&\leqslant \sum_i L_{2,i} |\theta_i - \theta'_i| \leqslant \max_i L_{2,i} \left\| \theta - \theta' \right\|_1 \leqslant \sqrt{m} \max_i L_{2,i} \left\| \theta - \theta' \right\|
\end{aligned}$$

[8] The constant L_2 can be given explicitly by bounding from below the support function of the inscribed ellipsoid of maximal volume, the so-called John ellipsoid. For symmetric convex bodies, L_2 can be made tightest possible. For simplicity, we avoid delving into these technicalities here.

as claimed. ∎

Appendix C. Proofs of section 4.

Proof of Proposition 3. Since (4.1) is the composition of Lipschitz continuous mappings of y by assumption, applying the chain rule [29, Theorem 4 and Remark, section 4.2.2] gives the formula. ∎

Proof of Proposition 4. The argument is exactly the same as that for Proposition 3, replacing y by θ where the required Lipschitz continuity assumptions with respect to θ hold true. ∎

Proof of Corollary 1. We first notice that $\mathcal{D}_a^{(\ell)} = (\mathcal{D}_\xi^{(\ell)}, \mathcal{D}_{z_1}^{(\ell)}, \dots, \mathcal{D}_{z_Q}^{(\ell)})$, where $\mathcal{D}_\xi^{(\ell)} = \partial_1 \xi^{(\ell)}(y,\theta)[\delta]$ and $\mathcal{D}_{z_k}^{(\ell)} = \partial_1 z_k^{(\ell)}(y,\theta)[\delta]$. Hence, applying again the chain rule [29, Theorem 4 and Remark, section 4.2.2] to the sequence of iterates and using the facts that all involved mappings are Lipschitz and $\mathcal{D}_x^{(\ell)} = \Gamma_a^{(\ell)}(\mathcal{D}_a^{(\ell)}) = \mathcal{D}_\xi^{(\ell)}$ conclude the proof. ∎

Proof of Corollary 2. Observe that $\mathcal{J}_a^{(\ell)} = (\mathcal{J}_\xi^{(\ell)}, \mathcal{J}_{z_1}^{(\ell)}, \dots, \mathcal{J}_{z_Q}^{(\ell)})$, where $\mathcal{J}_\xi^{(\ell)} = \partial_2 \xi^{(\ell)}(y,\theta)$ and $\mathcal{J}_{z_k}^{(\ell)} = \partial_2 z_k^{(\ell)}(y,\theta)$. Arguing as in the proof of Corollary 1, now using that $\mathcal{J}_x^{(\ell)} = \Gamma_a^{(\ell)}(\mathcal{J}_a^{(\ell)}) = \mathcal{J}_\xi^{(\ell)}$ yields the formula. ∎

Proof of Corollary 3. Argue as before, but now with $\mathcal{D}_a^{(\ell)} = (\mathcal{D}_\xi^{(\ell)}, \mathcal{D}_{\tilde{x}}^{(\ell)}, \dots, \mathcal{D}_u^{(\ell)})$, where $\mathcal{D}_\xi^{(\ell)} = \partial_1 \xi^{(\ell)}(y,\theta)[\delta]$, $\mathcal{D}_{\tilde{x}}^{(\ell)} = \partial_1 \tilde{x}^{(\ell)}(y,\theta)[\delta]$, $\mathcal{D}_u^{(\ell)} = \partial_1 u^{(\ell)}(y,\theta)[\delta]$, and $\mathcal{D}_x^{(\ell)} = \Gamma_a^{(\ell)}(\mathcal{D}_a^{(\ell)}) = \mathcal{D}_\xi^{(\ell)}$. The chain rule completes the proof. ∎

Proof of Corollary 4. Argue as before, but now with $\mathcal{J}_a^{(\ell)} = (\mathcal{J}_\xi^{(\ell)}, \mathcal{J}_{\tilde{x}}^{(\ell)}, \dots, \mathcal{J}_u^{(\ell)})$, where $\mathcal{J}_\xi^{(\ell)} = \partial_1 \xi^{(\ell)}(y,\theta)$, $\mathcal{J}_{\tilde{x}}^{(\ell)} = \partial_1 \tilde{x}^{(\ell)}(y,\theta)$, $\mathcal{J}_u^{(\ell)} = \partial_1 u^{(\ell)}(y,\theta)$, and $\mathcal{J}_x^{(\ell)} = \Gamma_a^{(\ell)}(\mathcal{J}_a^{(\ell)}) = \mathcal{J}_\xi^{(\ell)}$. The chain rule completes the proof. ∎

REFERENCES

[1] H. Attouch and B. F. Svaiter, *A continuous dynamical Newton-like approach to solving monotone inclusions*, SIAM J. Control Optim., 49 (2011), pp. 574–598.

[2] H. Avron and S. Toledo, *Randomized algorithms for estimating the trace of an implicit symmetric positive semi-definite matrix*, J. ACM, 58 (2011), 8.

[3] H. Bauschke and P. L. Combettes, *Convex Analysis and Monotone Operator Theory in Hilbert Spaces*, CMS Books Math./Ouvrages Math. SMC, Springer, New York, 2011.

[4] A. Benazza-Benyahia and J.-C. Pesquet, *Building robust wavelet estimators for multicomponent images using Stein's principle*, IEEE Trans. Image Process., 14 (2005), pp. 1814–1830.

[5] J. Bennett and S. Lanning, *The Netflix prize*, in Proceedings of KDD Cup and Workshop 2007, ACM, New York, 2007, pp. 3–6.

[6] T. Blu and F. Luisier, *The SURE-LET approach to image denoising*, IEEE Trans. Image Process., 16 (2007), pp. 2778–2786.

[7] T. T. Cai and H. H. Zhou, *A data-driven block thresholding approach to wavelet estimation*, Ann. Statist., 37 (2009), pp. 569–595.

[8] E. J. Candès and B. Recht, *Exact matrix completion via convex optimization*, Found. Comput. Math., 9 (2009), pp. 717–772.

[9] E. J. Candès, C. A. Sing-Long, and J. D. Trzasko, *Unbiased risk estimates for singular value thresholding and spectral estimators*, IEEE Trans. Signal Process., 61 (2013), pp. 4643–4657.

[10] A. Chambolle and T. Pock, *A first-order primal-dual algorithm for convex problems with applications to imaging*, J. Math. Imaging Vision, 40 (2011), pp. 120–145.

[11] C. Chaux, L. Duval, A. Benazza-Benyahia, and J.-C. Pesquet, *A nonlinear Stein-based estimator for multichannel image denoising*, IEEE Trans. Signal Process., 56 (2008), pp. 3855–3870.
[12] P. L. Combettes and J.-C. Pesquet, *A Douglas-Rachford splitting approach to nonsmooth convex variational signal recovery*, IEEE J. Sel. Topics Signal Process., 1 (2007), pp. 564–574.
[13] P. L. Combettes and J.-C. Pesquet, *Proximal splitting methods in signal processing*, in Fixed-Point Algorithms for Inverse Problems in Science and Engineering, Springer, New York, 2011, pp. 185–212.
[14] P. L. Combettes and V. R. Wajs, *Signal recovery by proximal forward-backward splitting*, Multiscale Model. Simul., 4 (2005), pp. 1168–1200.
[15] I. Daubechies, *Orthonormal bases of compactly supported wavelets*, Comm. Pure Appl. Math., 41 (1988), pp. 909–996.
[16] C.-A. Deledalle, V. Duval, and J. Salmon, *Non-local methods with shape-adaptive patches (NLM-SAP)*, J. Math. Imaging Vision, 43 (2012), pp. 103–120.
[17] C.-A. Deledalle, G. Peyré, and J. Fadili, *Stein COnsistent Risk Estimator (SCORE) for Hard Thresholding*, preprint, arXiv:1301.5874v1 [math.ST], 2013.
[18] C.-A. Deledalle, F. Tupin, and L. Denis, *Poisson NL means: Unsupervised non local means for Poisson noise*, in Proceedings of the 2010 17th IEEE International Conference on Image Processing, 2010, pp. 801–804.
[19] C.-A. Deledalle, S. Vaiter, G. Peyré, J. Fadili, and C. Dossal, *Proximal splitting derivatives for risk estimation*, J. Phys.: Conf. Ser., 386 (2012), 012003.
[20] C.-A. Deledalle, S. Vaiter, G. Peyré, J. Fadili, and C. Dossal, *Risk Estimation for Matrix Recovery with Spectral Regularization*, preprint, arXiv:1205.1482v3 [math.OC], 2012.
[21] C.-A. Deledalle, S. Vaiter, G. Peyré, J. Fadili, and C. Dossal, *Unbiased risk estimation for sparse analysis regularization*, in Proceedings of the 2012 19th IEEE International Conference on Image Processing, 2012, pp. 3053–3056.
[22] S. J. Dong and K. F. Liu, *Stochastic estimation with Z_2 noise*, Phys. Lett. B, 328 (1994), pp. 130–136.
[23] D. L. Donoho and I. M. Johnstone, *Adapting to unknown smoothness via wavelet shrinkage*, J. Amer. Statist. Assoc., 90 (1995), pp. 1200–1224.
[24] C. Dossal, M. Kachour, M. J. Fadili, G. Peyré, and C. Chesneau, *The degrees of freedom of the lasso for general design matrix*, Statist. Sinica, 23 (2013), pp. 809–828.
[25] V. Duval, J.-F. Aujol, and Y. Gousseau, *A bias-variance approach for the nonlocal means*, SIAM J. Imaging Sci., 4 (2011), pp. 760–788.
[26] A. Edelman, *Jacobians of Matrix Transforms (with Wedge Products)*, Handout 3, MIT, Cambridge, MA, 2005.
[27] B. Efron, *How biased is the apparent error rate of a prediction rule?*, J. Amer. Statist. Assoc., 81 (1986), pp. 461–470.
[28] Y. C. Eldar, *Generalized SURE for exponential families: Applications to regularization*, IEEE Trans. Signal Process., 57 (2009), pp. 471–481.
[29] L. C. Evans and R. F. Gariepy, *Measure Theory and Fine Properties of Functions*, CRC Press, Boca Raton, FL, 1992.
[30] M. Fazel, *Matrix Rank Minimization with Applications*, Ph.D. thesis, Department of Electrical Engineering, Stanford University, Stanford, CA, 2002.
[31] D. Gilbarg and N. S. Trudinger, *Elliptic Partial Differential Equations of Second Order*, 2nd ed., Classics Math. 517, Springer-Verlag, Berlin, 1998.
[32] D. A. Girard, *A fast "Monte Carlo cross-validation" procedure for large least squares problems with noisy data*, Numer. Math., 56 (1989), pp. 1–23.
[33] R. Giryes, M. Elad, and Y. C. Eldar, *The projected GSURE for automatic parameter tuning in iterative shrinkage methods*, Appl. Comput. Harmon. Anal., 30 (2011), pp. 407–422.
[34] G. H. Golub, M. Heath, and G. Wahba, *Generalized cross-validation as a method for choosing a good ridge parameter*, Technometrics, 21 (1979), pp. 215–223.
[35] A. Griewank and A. Walther, *Evaluating Derivatives: Principles and Techniques of Algorithmic Differentiation*, SIAM, Philadelphia, 2008.
[36] J.-B. Hiriart-Urruty and C. Lemaréchal, *Convex Analysis and Minimization Algorithms*, Vols. I–II, Springer-Verlag, Berlin, 2001.
[37] H. M. Hudson, *A natural identity for exponential families with applications in multiparameter estimation*, Ann. Statist., 6 (1978), pp. 473–484.

[38] H. M. Hudson and T. Lee, *Maximum likelihood restoration and choice of smoothing parameter in deconvolution of image data subject to Poisson noise*, Comput. Statist. Data Anal., 26 (1998), pp. 393–410.
[39] M. F. Hutchinson, *A stochastic estimator of the trace of the influence matrix for Laplacian smoothing splines*, Comm. Statist. Simulation Comput., 18 (1989), pp. 1059–1076.
[40] K. Kato, *On the degrees of freedom in shrinkage estimation*, J. Multivariate Anal., 100 (2009), pp. 1338–1352.
[41] N. Komodakis and J.-C. Pesquet, *Playing with Duality: An Overview of Recent Primal-Dual Approaches for Solving Large-Scale Optimization Problems*, preprint, arXiv:1406.5429v1 [cs.NA], 2014.
[42] A. S. Lewis and M. L. Overton, *Nonsmooth optimization via quasi-Newton methods*, Math. Program., 141 (2013), pp. 135–163.
[43] A. S. Lewis and H. S. Sendov, *Twice differentiable spectral functions*, SIAM J. Matrix Anal. Appl., 23 (2001), pp. 368–386.
[44] K.-C. Li, *From Stein's unbiased risk estimates to the method of generalized cross validation*, Ann. Statist., 13 (1985), pp. 1352–1377.
[45] F. Luisier, T. Blu, and M. Unser, *SURE-LET for orthonormal wavelet-domain video denoising*, IEEE Trans. Circuits Syst. Video Technol., 20 (2010), pp. 913–919.
[46] S. Mallat, *A Wavelet Tour of Signal Processing. The Sparse Way*, 3rd ed., Elsevier/Academic Press, Amsterdam, 2009.
[47] U. Naumann, *Optimal Jacobian accumulation is NP-complete*, Math. Program., 112 (2008), pp. 427–441.
[48] J.-C. Pesquet, A. Benazza-Benyahia, and C. Chaux, *A SURE approach for digital signal/image deconvolution problems*, IEEE Trans. Signal Process., 57 (2009), pp. 4616–4632.
[49] J.-C. Pesquet and D. Leporini, *A new wavelet estimator for image denoising*, in Proceedings of the Sixth International Conference on Image Processing and Its Applications, IET, Stevenage, UK, 1997, pp. 249–253.
[50] H. Raguet, J. Fadili, and G. Peyré, *A generalized forward-backward splitting*, SIAM J. Imaging Sci., 6 (2013), pp. 1199–1226.
[51] S. Ramani, T. Blu, and M. Unser, *Monte-Carlo SURE: A black-box optimization of regularization parameters for general denoising algorithms*, IEEE Trans. Image Process., 17 (2008), pp. 1540–1554.
[52] S. Ramani, Z. Liu, J. Rosen, J.-F. Nielsen, and J. A. Fessler, *Regularization parameter selection for nonlinear iterative image restoration and MRI reconstruction using GCV and SURE-based methods*, IEEE Trans. Image Process., 21 (2012), pp. 3659–3672.
[53] S. Ramani, J. Rosen, Z. Liu, and J. A. Fessler, *Iterative weighted risk estimation for nonlinear image restoration with analysis priors*, in Proceedings of SPIE, Vol. 8296, Computational Imaging X, SPIE, Bellingham, WA, 2012, 82960N.
[54] M. Raphan and E. P. Simoncelli, *Optimal denoising in redundant representations*, IEEE Trans. Image Process., 17 (2008), pp. 1342–1352.
[55] M. Raphan and E. P. Simoncelli, *Least squares estimation without priors or supervision*, Neural Comput., 23 (2011), pp. 374–420.
[56] J. Rice, *Choice of smoothing parameter in deconvolution problems*, Contemp. Math., 59 (1986), pp. 137–151.
[57] R. T. Rockafellar, *Monotone operators and the proximal point algorithm*, SIAM J. Control Optim., 14 (1976), pp. 877–898.
[58] F. Roosta-Khorasani and U. Ascher, *Improved Bounds on Sample Size for Implicit Matrix Trace Estimators*, preprint, arXiv:1308.2475 [cs.NA], 2013.
[59] L. I. Rudin, S. Osher, and E. Fatemi, *Nonlinear total variation based noise removal algorithms*, Phys. D, 60 (1992), pp. 259–268.
[60] X. Shen and J. Ye, *Adaptive model selection*, J. Amer. Statist. Assoc., 97 (2002), pp. 210–221.
[61] V. Solo and M. Ulfarsson, *Threshold selection for group sparsity*, in Proceedings of the 2010 IEEE International Conference on Acoustics, Speech and Signal Processing, 2010, pp. 3754–3757.
[62] C. M. Stein, *Estimation of the mean of a multivariate normal distribution*, Ann. Statist., 9 (1981), pp. 1135–1151.
[63] D. Sun and J. Sun, *Nonsmooth Matrix Valued Functions Defined by Singular Values*, Technical report, Department of Decision Sciences, National University of Singapore, Singapore, 2003.

[64] R. J. Tibshirani and J. Taylor, *The solution path of the generalized lasso*, Ann. Statist., 39 (2011), pp. 1335–1371.
[65] R. J. Tibshirani and J. Taylor, *Degrees of freedom in lasso problems*, Ann. Statist., 40 (2012), pp. 1198–1232.
[66] S. Vaiter, C.-A. Deledalle, G. Peyré, C. Dossal, and J. Fadili, *Local behavior of sparse analysis regularization: Applications to risk estimation*, Appl. Comput. Harmon. Anal., 35 (2013), pp. 433–451.
[67] S. Vaiter, C.-A. Deledalle, G. Peyré, J. M Fadili, and C. Dossal, *The Degrees of Freedom of Partly Smooth Regularizers*, preprint, arXiv:1404.5557v2 [math.ST], 2014.
[68] D. Van De Ville and M. Kocher, *SURE-based non-local means*, IEEE Signal Process. Lett., 16 (2009), pp. 973–976.
[69] D. Van De Ville and M. Kocher, *Non-local means with dimensionality reduction and SURE-based parameter selection*, IEEE Trans. Image Process., 9 (2011), pp. 2683–2690.
[70] C. Vonesch, S. Ramani, and M. Unser, *Recursive risk estimation for non-linear image deconvolution with a wavelet-domain sparsity constraint*, in Proceedings of the 15th IEEE International Conference on Image Processing, 2008, pp. 665–668.
[71] J. Ye, *On measuring and correcting the effects of data mining and model selection*, J. Amer. Statist. Assoc., 93 (1998), pp. 120–131.
[72] M. Yuan and Y. Lin, *Model selection and estimation in regression with grouped variables*, J. R. Stat. Soc. Ser. B Stat. Methodol., 68 (2006), pp. 49–67.
[73] H. Zou, T. Hastie, and R. Tibshirani, *On the "degrees of freedom" of the lasso*, Ann. Statist., 35 (2007), pp. 2173–2192.